Palacký University Olomouc

Faculty of Science

Department of Geology

Hydrocarbons in Lower Devonian carbonates of Prague Basin and stylolites as possible pathways for petroleum migration

Bachelor thesis

Sajjad Akram Murad Hawasi

Petroleum Engineering (B0724A330002)

Fulltime study

Supervisor: Prof. Mgr. Ondřej Bábek, Dr.

Olomouc 2023

Hydrocarbons in Lower Devonian carbonates of Prague Basin and stylolites as possible pathways for petroleum migration

Anotace:

Tato práce se zabývá zkoumáním uhlovodíků v karbonátech spodního devonu nacházejícími se v pražské pánvi, přičemž objasňuje geologické a geochemické aspekty, které ovlivňují jejich přítomnost a distribuci. Karbonátové formace spodního devonu jsou významné díky svému potenciálu jako zásobárny uhlovodíků. Studie zdůrazňuje klíčovou roli, kterou stylolity, nepravidelné, vlnité, mineralizované v horninách při migraci ropy. Tyto stylolity mohou potenciálně působit jako nekonvenční potrubí pro ropné tekutiny, ovlivňující pohyb a akumulaci uhlovodíků. Podrobné geologické mapování, shromažďování vzorků hornin a geochemická analýza k doložení jejich tvrzení a nabízí pohledy, které by mohly změnit chápání migrace uhlovodíků a optimalizace nádrží. Tento dokument může sloužit jako cenný zdroj pro geology, ropné inženýry a další průmyslové profesionály, kteří se zajímají o průzkum a produkci uhlovodíků.

Klíčová slova: Gama záření, uhlovodíky, uhličitany spodního devonu, pražská pánev, stylolity, migrace ropy

Počet stran: 53
Počet příloh: 0

Anotation:

This Thesis delves into the examination of hydrocarbons in the Lower Devonian carbonates located in the Prague Basin, illuminating the geological and geochemical aspects that impact their presence and distribution. The Lower Devonian carbonate formations are significant due to their potential as hydrocarbon reservoirs. The study emphasizes the crucial role that stylolites, irregular, wavy mineralized within rocks in petroleum migration. These stylolites can potentially act as unconventional conduits for petroleum fluids, influencing the movement and accumulation of hydrocarbons. The detailed geological mapping, rock sample collection, and geochemical analysis to substantiate their claims, offering insights that could reshape understandings of hydrocarbon migration and reservoir optimization. This paper may serve as a valuable resource for geologists, petroleum engineers, and other industry professionals interested in hydrocarbon exploration and production.

I declare that I have prepared the bachelor's thesis myself and that I have stated all the used information resources in the thesis.

In Olomouc, July 27, 2022 ....

Sajjad Hawasi

Acknowledgement

Through writing my Thesis, I was given a fantastic amount of help and support. First and foremost, I would like to thank my supervisor "Dr. prof. Mgr. Ondřej Bábek, Dr." for his assistance. The knowledge provided was key to developing the study questions and methods. Your Insightful feedback encouraged me to improve my approach and moved my effort to a higher level.

I would like to thank all Palacky University faculty members from the Department of Geology, Petroleum Engineering, and Soran University for assisting me during my studies and research and for their invaluable assistance and support throughout the laboratory work.

In addition, I'd like to express my very great appreciation, to my parents, specifically my mother and father, for their sensible advice and unending support. You've always been there for me in hard times. Finally, I could not have finished this without the help of my friends and siblings, who provided intellectual talks and pleasurable distractions from my study. Thank you all for inspiring me to do greater.

Contents

List of graphic

1. Chapter 1 - Introduction and Objectives

1.1 Introduction

The Prague Basin is located in the Teplá–Barrandian area within the Czech Republic. It is about 65 km and stretches between the cities of Prague and Pilsen. It represents a famous location for the Lower and Middle Paleozoic periods in Europe. The Prague Basin contains a very significant geological structure and many fossil records. (Mergl, 2011).

The Barrandian region or area has been commonly known by this name for more than a century. Barrandian region is classified as "unmetamorphosed" and poorly metamorphic Proterozoic and Paleozoic strata (Cambrian to Devonian) in Central and Western Bohemia. (Chlupáč and Štorch 1992)

The sedimentary rock formation of the Prague Basin covers many time geological periods, ranging from the Late Proterozoic through the Cretaceous, including the fact that the Lower Devonian period is part of the early Paleozoic time period as well, and its sediments are actually a component of the Prague Basin's geological structure itself. In the Prague Basin, it has been known for a very long time that there are bitumen occurrences in outcrops. However, there are no economic hydrocarbon accumulations have been found at the Prague Basin even though the existence of bitumen and petroleum inclusions is considered strong evidence of the generation, migration, and movement of hydrocarbons throughout the basin. (Jahn, 1883).

Bitumens were exclusively discovered in the Silurian and Devonian strata, where they were housed and trapped in veins, fossil molds, or even inside the vuggy porosity. Therefore, the migration and movement of the hydrocarbon was confined only to the faults and fracture systems due to the reason that the Prague Basin has no carrier systems nor reservoirs of any kind to store the hydrocarbon. (Volk, 2000).

In addition, petroleum inclusions have been discovered in syntaxial spread cements on organism fragments, and hydrocarbons have been detected in the pore space during cementation. As a result, the Scyphocrinites horizon is the only recognized potential carrier rock in the Prague Basin. However, the high concentration of bitumen and

petroleum particles in fractures and stylolites shows that fracture migration is more important than the migration in pore space.

According to recent studies, observations, and simulations, the permeability of stylolites is considered as anisotropic, thus the stylolites may operate as both seals and fluid channels or pathways depending on the substance that was collected in the stylolite itself. (Koehn et al, 2016).

The Scyphocrinites horizon has been identified as the only known probable carrier rock in the Prague Basin based on the observed distribution of bitumen and petroleum components. However, the high abundance of bitumen and petroleum inclusions in fractures and stylolites indicates that migration via fractures plays a more important part than migration through pores.(Volk, 2000).

1.2 Research Objectives

The aim of this thesis was to establish link of the bitumen occurrence with stratigraphy and petrology of the host carbonates of the Lochkov Formation, and compared it with the overlying Praha Formation in the Prague Basin. In specifically, the concentration of bitumens in pressure-dissolution structures, also known as stylolites, of comparatively pure carbonates was investigated with the purpose of determining whether or not stylolites might serve as potential paths for the migration of hydrocarbons. For the next step, the total organic carbon (TOC), total inorganic carbon TIC), and total sulfur (TS) analysis was used for identifing the stratigraphic zones enriched in hydrocarbons in Lower Devonian rocks of the Prague Basin (Lochkov Formation) including using the data of U/Th ratios that was recorded from gamma-ray spectrometry at both selected outcrop sections, then linking the hydrocarbon enriched zones with distribution of stylolites as well as using thin-section petrographic analysis and fluorescence microscopy for analysing the macroscopic features of carbonate rocks, and finally, the organic-geochemistry techniques such as biomarker and gas chromatography was used for identifying the types and genesis of bitumens inside each sample.

2. Chapter 2 – Background and Literature Review: Organic matter in sedimentary rocks and its migration

Sedimentary rocks, in particular, are significant because they serve as organic matter reservoirs. The bulk of organic matter (OM) originates from the fossilized remains of animals trapped in sediment, such as plants and plankton.

These fossils might be discovered in the silt. Because the presence of organic matter in sedimentary rocks is required for the formation of hydrocarbons, these rocks are critical for the exploration and extraction of fossil fuels.

This organic material is ultimately turned into oil and natural gas as a consequence of diagenesis and catagenesis processes, which take a long time and may occur both within and between rock layers.

The generation of petroleum from organic-rich rocks is caused by the burial of these source rocks in the temperature and pressure of the oil and gas window, and this results in the source rocks being subjected to conditions that are suitable for the production of petroleum (Tissot & Welte, 1984).

Carbon analysis test is considered as one of very important analytical method for studying the organic matter. It is the process of measuring and quantifying 3 main types of carbon in a sample, which are the Total Organic Carbon (TOC), which is used for analysing carbon components in samples that contains organic materials such as plant remnants, animal remains, and microbial biomass, therefore, it focuses on studying any samples contains organic carbon.

However, the Total Inorganic Carbon (TIC) which is sused for analysing the amount of inorganic carbon that can be found in a sample (Carbonates and bicarbonates are the most common examples), and it is used usually for testing the carbonate-rich minerals, rocks, or the aquatic carbon cycle. Finally, the Total Carbon (TO), which is the total amount of all carbon that can be existed in a sample, whether it is organic or inorganic.

3. Chapter 3: Geological settings and stratigraphy of the Prague Basin

The Prague Basin is an infilling of a tectonically predisposed, narrow linear valley that is located in the center of Bohemia, and it has its highest thickness and its deepest section along with its central horizontal axis.(Havlíček1981, 1982). Its boundary is known as a significant stratigraphic boundary of the Early Devonian Period

The Prague Basin represents the central portion of the geological Teplá-Barrandian unit (TBU) of the Bohemian Massif, which has been defined by Neoproterozoic (Cadomian) basement and overlain by Lower Paleozoic (Cambrian - Middle Devonian) as a result of volcanic-sedimentary sequences.(Vodrážková et al., 2022).

Throughout the history of the Prague Basin, the evolution of its facies was influenced by global and regional factors, along with local tectonic circumstances and settings. (Havlíček 1981, and Chlupáč & Kukal 1988). The north-western side location of the Prague Basin has shallow water sediments, and some certain areas are even being periodically appeared above the sea surface. On the other hand, the south-eastern part of the Prague Basin can be defined as comparatively deeper water facies. (Kukal 1957).

The coordinate system that is currently used for Basin has longest axis of the structure goes nearly to the direction of NE to SW, and it is a denudation remnant stretching approximately 100 kilometers from Starý Plzenec in the southwest to Úvaly near Prague in the northeast (Havlíček 1981). The Prague Basin according to an interpretation, was opened up as a rift basin during the early Ordovician geological time period, as a reaction to the extension that occurred over the peri–Gondwana area. (Žák et al. 2013).

The orogen of dissected Cadomian serves as the source region for the shallow-marine siliciclastics that were deposited in the subsequent Prague Basin during the Ordovician period. (Patočka & Štorch, 2004). Prague Basin itself was formed due to the reason of an erosion from the unmetamorphosed Lower Ordovician until the volcano-sedimentary rocks of the Middle Devonian. (Cháb, 2010).

During the Late Devonian to the early Carboniferous Variscan orogeny, the basin was inverted and for multiple times was damaged, therefore, its inventory of structure was characterized by a syncline that has been cut through by thrust faults or reverse. (VACEK, and ŽÁK, 2017). A noticeable band of red pelagic carbonate that is up to around 15 meters of thickness can be connected over many tens of kilometers may be seen in the Lower Devonian (Pragian) carbonate layers which makes up the Prague Formation in the Prague Basin in the Czech Republic.(Bábek et al., 2018).

The Lower and Middle Devonian (Lochkovian to Givetian) in the Prague Basin in the Czech Republic, was characterized by a sequence of large deep-sea carbonates and shales that had a typical lifetime of around 5–7 million years. (Šimíček et al., 2020)
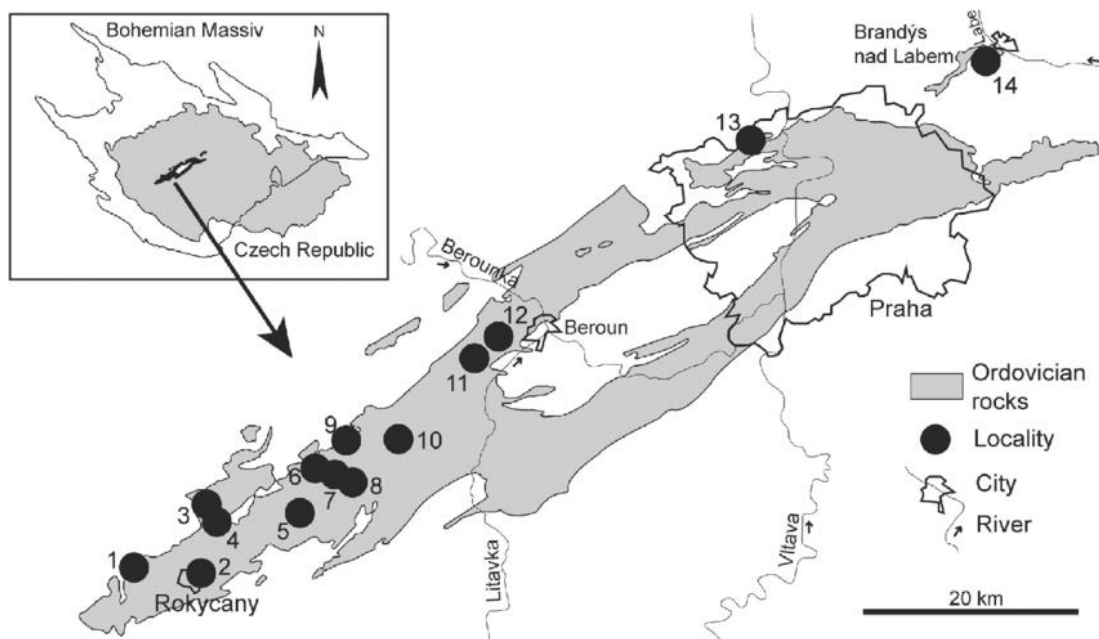
Figure 1: Prague Basin, Czech Republic (Aubrechtova et al., 2015).

4. Chapter 4: Materials and Methodology

4.1. Measuring the gamma-ray spectrometer at the selected outcrop sections.

The first experimental procedure before using the gamma-ray spectrometer equipment, was to measure the thickness of each layer at both field-locations in the Prague Basin in the Czech Republic, the Velka Chuchle section, which is located based on the coordination (50.0147278N,14.3732447E), and at the NaChlumu Quarry section with coordination of (49.9462678N,14.1332514E).

The next step, was by using a normal measuring-tape inorder to put a mark or label every 50 cm on a well flat surface of every possible layer. Therefore, the first layer on the ground representis the mark of zero-point, and it is geologically called an underlying bedrock.

After the preparation process, the Gamma-ray spectrometer equipment was used for every layer that was marked during the preparation. The spectrometer equipment that was used is RS-230 Super Spec portable spectrometer with $2''\times2''$ (103 ccm) bismuthgermanate scintillation detector.

The spectrometer equipment were fixed on the flat surface of each layer that was already marked during the preparation, and then after waiting for almost 180 s (3 minutes, for recording each layer), the spectrometer successfully recorded the logged data for the layer.

Finally, The device converted the recorded data from per second, in selected energy windows, to concentrations of K with unit of (%), U with unit of (ppm), and Th with unit of (ppm), as well as the rate of dose with unit of (nGy/h).(Bábek et al, 2013).

Figure 2: Using the gamma-ray spectrometer equipment at the Field

4.2.   Field-Samples collection

Samples were all taken from each layer by using a geological hammer for the purpose of laboratory analysis such as the core-plug analysis, thin-section analysis, and more. Stratigraphically, the samples belong to the Lower Devonian limestones, so by using a small hand lense to take a closer look at structure of rocks in the field which helps identifying some minerals and fossils in samples, the shape, brightness, color, and cleavages.

Therefore, the rock samples from each layer were described as calcarenite rocks, with light gray color, and they all were medium grained with calcite veins. In addition, The number of samples from Velka Chuchle section was 5 samples, while 8 samples

from the Na Chlumu Quarry section. In addition, all of the samples were stored, labeled and then taken to laboratory for the purpose of analysis.
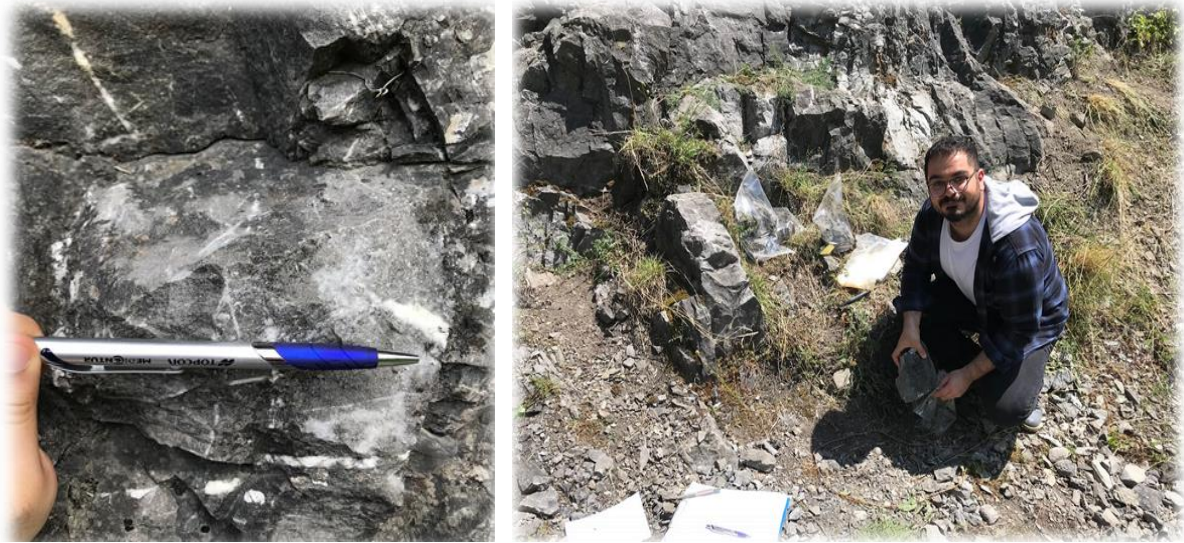
Figure 3: Collecting Samples from the field, so they will be used for analysis processes in lab.

4.3. Core plug preparation

The core-plug samples were drilled and taken from large rock samples that were collected and collected from both field locations, Velka Chuchle, and Na Chlumu Quarry. These rock samples were taken not randomly but specifically from the layers that were previously measured and logged by the gamma-ray spectrometer, in order to be studied and analyzed in the laboratory and connected its date with other analytical processes or methods.

The rock samples were first cut in the laboratory, by a special electrical machine that is called Rock Trim-Saw, which has a circular saw that runs by an electrical motor in order to provide a very high rotation rate which is required to cut the rock due to its high hardness, and it also has a water-cooling system which is important due to the temperature increasing during the cutting process. Eventually, the rock samples were used for extracting the core-plugs successfully, and prepared for the laboratory.

Figure 4: Preparing Core-Plugs from the rock samples

4.4. Thin-section preparation

This-section analysis, also known as Morphological Analysis (MA), which is a very important laboratory method for researching and investigating the entire properties of rock samples. Therefore, the thin sections were cut off, extracted, and then prepared from the same rock samples that used for the core-plugs preparation.

After that, all these small rock samples were glued to a thin glass slide by using epoxy resin, which is a chemical material used most commonly for sticky purposes due to its very strong properties. Then, the overflowing part of rock was also cut off by using a saw.

Figure 5: Preparing Thin Sections from the rock samples from field.

After that, the thin sections were prepared for the polishing process by using a hand polishing first, then an electric polishing machine with diamond paste solution,

which is a liquid compound used for the purpose of polishing the surfaces of materials such as rocks and stones, so the final thickness of all thin sections was moreover to 0.04 mm, after finishing with the polishing process and its diamond paste solution with grossness of 1/4 microns for the first 3-5 minutes.

Figure 6: Polishing every samples for thin-section

Eventually, all of the thin-section samples after finishing the polishing process, became ready and prepared very well for the microscope digital photography analysis, and then for the petrographic analysis using a (FL) Fluorescence Microscopy.
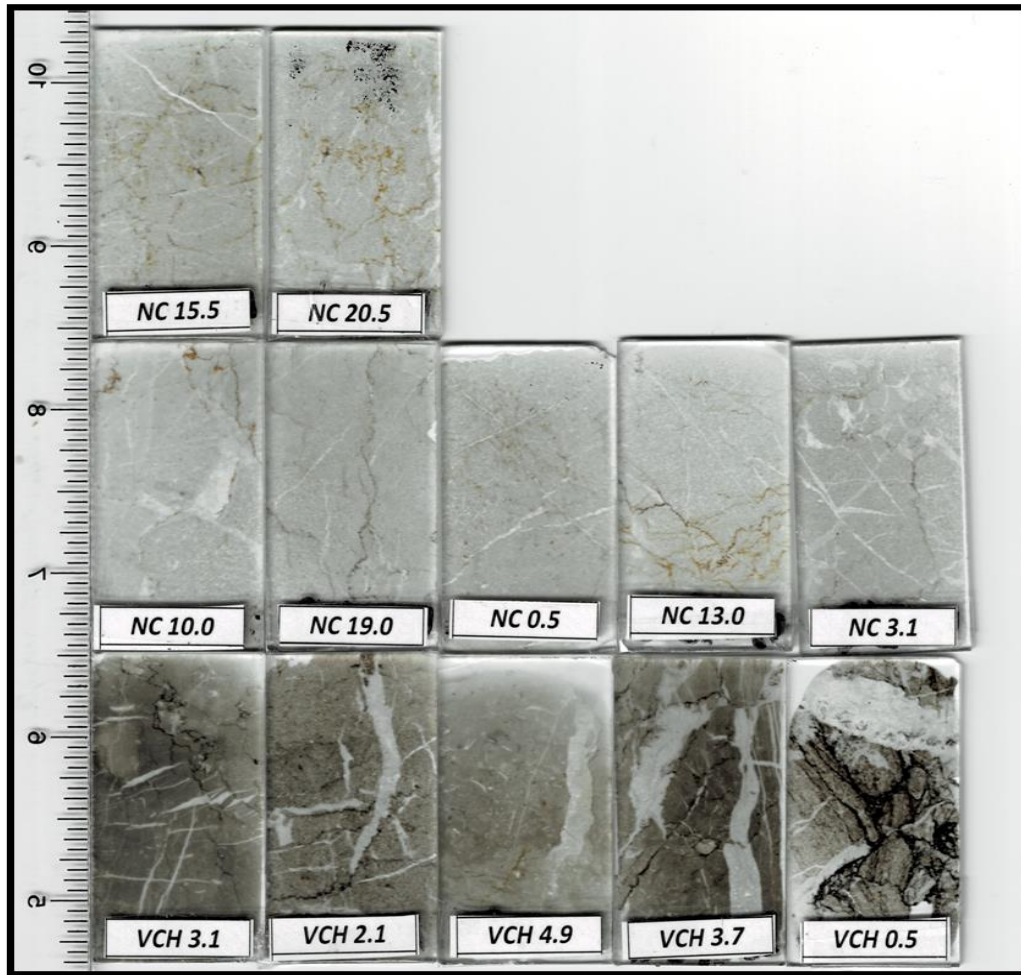
Figure 7: thin-section samples after polishing

4.5. Powder samples preparing

Analyzing the powder of each rock sample is considered as a significant and very important analytical methodology, because it allows later to measure the important properties inside each rock sample by using the Gas chromatography (GC) analytical technique, which is a serious analytical method by special laboratory devices in order to identify the chemical components of each mixture powder sample, and to define the existence of the component including the amount of it, including using biomarkers techniques of rocks.

The first step of changing each rock samples into powder, is by using YX-ZM100 grinding machine, which is a laboratory machine used specifically for grinding

rock samples into powder. This device is very commonly used in geology laboratory, mining laboratory, and chemical laboratories.

The machine consists of a heavy metallic pot where the rock sample was put inside, and another heavy thick metallic ring-shaped object with a small heavy disk, which they all work together as a heavy hummer that eventually leads to crushing the rock sample inside it due to the high vibration and high-speed spinning the machine already generates by a special electric motor equipment inside it.

Figure 8: Rocks grinding equipment in lab

After waiting for 5 minutes, the rock powder was ready, so we stopped the machine by pressing its red bottom, and we carefully opened it, and picked up the heavy metallic pot. Then, by using a soft brush, we gathered all the powder in a small plastic bag containing a label of the rock sample details so we can later know which layer it belonged to during the next step of laboratory powder analysis work.
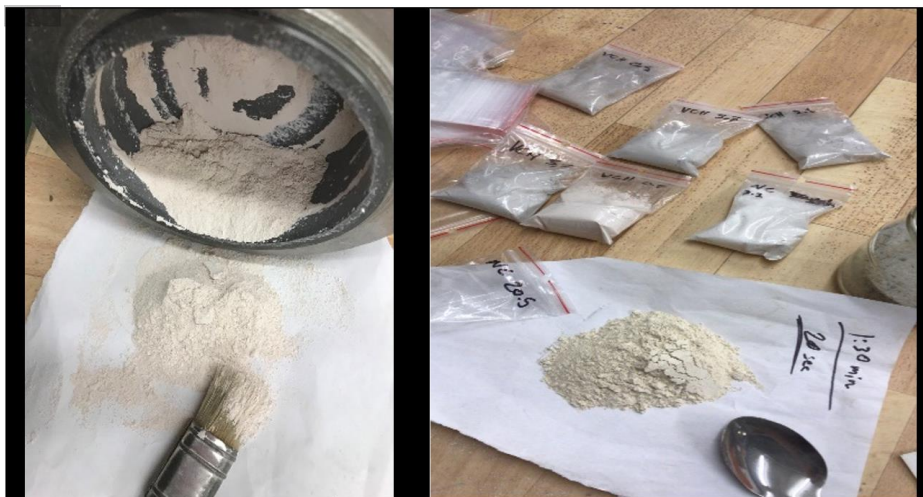
Figure 9: rock samples become powder for chemical analysis

4.6. Soxhlet

Since the majority of carbonate reservoir rocks are from the beginning oil-wet, therefore the Soxhlet Extractor, which is a piece of an equipment used in laboratories, was used to extract and remove any water, oil, or any liquid from each core sample. So, all the core-plug samples in the early stages, were cleaned very well by using Toluene within the Soxhlet Extractor equipment for 2 days.

During this process, a colourless outflowing was acquired which was a sign that all the oil residual from the core-plugs samples were completely removed. The next step of the cleaning process was using the Methanol for 3 days, and this step was important to remove any salts could be existed inside the samples which cannot be removed by using the Toluene during the first cleaning process.
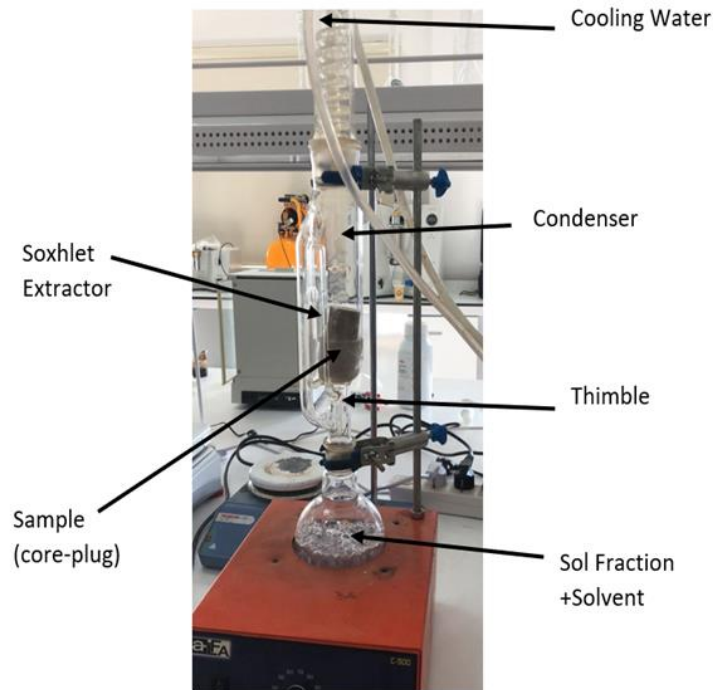
Figure 10: Soxhlet for cleaning core plugs before measuring porosity and permeability

Finally, after the cleaning process was finished, the core-plug samples were then putted inside oven machine for around two days, so they can be dry at temperature of 70 °C. Finally, all the core-plugs were cleaned from oil, salt, or any components and they all prepared and ready for the next laboratory step of measuring porosity and permeability.

4.7.   Porosity measurement

A rock's porosity is known as a percentage of its overall volume and the ratio of its pores, voids, and spaces. Most hydrocarbon reservoirs are made out of the sedimentary rocks, which typically means they have porosity values ranging are between 10-40% for the sandstone rocks, while the porosity values ranging are between 5-25% for the carbonate rocks. So, the sandstone rock has the ability to store and hold high mount of fluids inside it due to its high porosity percentage structure.

On the other hand, the carbonite rocks have a different and less pore structure system, therefore its porosity is less than the sandstone, but it is still considered as good porosity percentage.

The equation that is used to measure the porosity:

$$\phi = \frac{V_{pore}}{V_{bulk}}$$

ϕ: porosity (%)

Vpore: pore-volume (cm3)

Vbulk: bulk-volume (cm3)

Generally, there are three main categories of porosity. The first type is the Primary Porosity, which is defined as the total percentage of all the empty spaces and pores inside the rock that were fundamentally existed from the beginning of the rock formatting. Another type is called the Secondary Porosity, which is known and defined as the number of all spaces and pores inside the rock that were developed after the rock was formed, so it existed in rocks but after a long while, and as an example of that are the cracks or fractures that can be seen inside some rocks.

A porosimeter device used to measure the porosity of each core plug samples after the preparation. This laboratory analytical method requires either extracting a fluid from the rock or injecting a fluid into the pore spaces inside the rock. To eliminate the residual hydrocarbon, the samples were washed with dichloromethane liquid and dried during using the Soxhlet previous lab process. The porosimeter successfully identified the porosity percentage as a calculated written data including the general parameters of each core samples, including core weight, length, diameter, pore volume with the porosity itself.

4.8. Permeability measurement

Measuring the permeability of each core-plug samples, was done by using a Gas Permeameter machine, with the standards and specifications of Model: MP-02. Permeability Range: 1-500 mD.
This device has a chamber which is a core-sample holder that is made of steel. Each core-plug sample was putted inside the chamber individually, one by one, and then the top of the chamber was closed very perfectly preventing any type of leaks.

The injection pressure was set by using a small electronic screen on the machine itself. Then, a Nitrogen Gas was injected through each core-plug sample, but individually. Then, the flowrate was measured by the device itself automatically and also for each core-plug sample. The measurements for all of the core plugs, were carried out with a confining pressure that is similar to a real reservoir pressure, a zero-back pressure, and a temperature of 25 C°.

Under steady-state circumstances of fluid flow, the permeameter provided the real value of liquid permeability. In each core-plug sample, the differential pressure (P), which its results come from the entrance and output pressures, has been continually measured. Using the Darcy Law, the permeability's magnitude was also determined.

Figure 11: Measuring the permeability

4.9. XRF (X-ray fluorescence) analysis

XRF (x-ray Fluorescence) analysis is considered as a powerful analytical technique for determining a material's elementals and especially the compositions of rock samples. It offers useful and valuable readings and details regarding the concentration of many different elements in a sample. XRF analysis is very quiet used in many several industrial and scientific applications because of its results and the simple requirement of using it.

The XRF analysis technique is used in many applications such geology, mining, materials science, environmental studies, and pharmaceutical products. It works based on the interaction that happens between x-rays that is generated from the device itself and the atoms inside a sample.

Figure 12: X-ray fluorescence device in lab

For the solid samples, they were crushed and grinded perfectly created a dry powder from each rock sample because reducing the size of particle will increase the sample surface area including its homogeneity.

Next, each sample was positioned in the XRF instrument's sample chamber, then an x-ray was directed and sent to the sample surface, so the emitted x-ray photons from the sample itself were immediately detected by the device including its wavelength and amount of energy for each photon sent out from the sample, therefore these information and data was used by the machine's computer to identify the type of elements with the percentages inside every samples.

4.10. TOC, TIC, TS analysis

The process elemental analysis (TOC, TIC, TS) for all the powdered samples, the device ELTRA 2000 that is equipped with 3 infrared detectors, was used at (Czech Geological Survey in Brno). First analysis (TIC) step, was done successfully by measuring the total inorganic carbon (TIC) after the carbon dioxide gas (CO2) was produced and generated due to using Phosphoric acid treatment for the samples from the beginning.

The next step of measuring the both total organic carbon (TOC) and total sulfur (TS), were also done successfully by removing the carbonate minerals using HCL acid treatment at temperature of 40°C on a hot plate followed with oxidation process at 1350°C in oxygen flow.

Figure 13: ELTRA 2000, TOC, TIC, TS Analysis device

In addition, for measuring the (TS), contains of three main steps, the preparation of the sample, which is very considerable for achieving better results of burning during combustion process, thus it was very important that the samples be grinded well enough before the oxidation process (burning) as well as the combustion or (oxidation) process, which was done by using high temperature in the presence of O2 for in order to converted all the sulfur inside the sample into sulfur dioxide gas (SO2), so later it causes

the detection the (SO2) sulfur Dioxide itself after being generated, and it was also done and recorded successfully.

4.11. Fluorescence microscopy analysis for thin-sections

Thin-Section petrographic analysis Using a (FL) Fluorescence Microscopy is an advanced optical microscope, that is using fluorescence and phosphorescence light rather than the reflection of the visible light.

The method of fluorescence microscopy is commonly used in the laboratory for petrographic analysis and studies because it can easily show the spots or area of the organic matter compounds inside the thin section sample.

In summary, when radiation hits the thin section sample, the electrons inside the atoms of this sample will receive this high energy, and therefore it forces the electrons to jump to a high orbital level inside the atom, which then, the electrons will return back to their original orbital level (lower), thus this process makes the electrons emit special light, which is the reason it is used to investigate the characteristics of organic substances compounds inside thin-section, including other study areas like to analyze the micropores, voids distribution, and microfractures, because once any organic chemical molecules exposed to fluorescence radiation, they will release light with a special color.
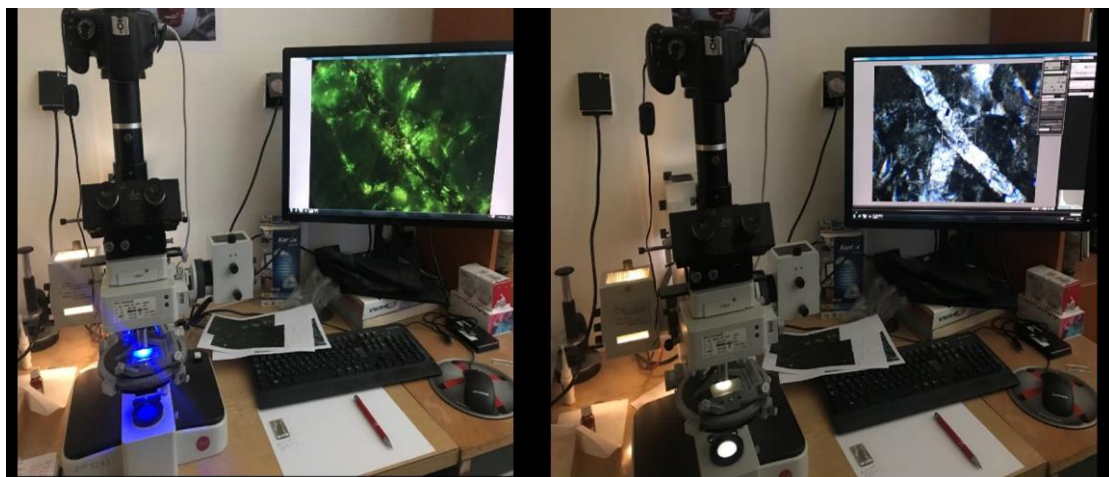
Figure 14: Fluorescnce Microscope for thin-sections

First of all, each thin-section sample was placed one after one in a specific place named Stage located under the objective of the Fluorescence Microscope, then the device was electrically switched-on. Safety steps are very necessary when using the Fluorescence Microscope due to the damage and harm that it can create due to its high-energy, therefore the next important step was to change the emission filter from number1 to number 3, by rotating a small metallic disc located above the objective and the nose piece.

The Dichroic filter is a thin special filter inside the Fluorescence Microscope equipment, and it is designed to allow only a specific wavelength of light to pass through it while reflecting other light waves. After that, the small metallic white lever on the left side of the Microscope has been lowered down, which is very important to change the prism mirror angle inside the microscope, and send the light to the digital camera output instead of the observation tubes. Next, a small black lever has been raised up, which is connected to the excitation filter that allows the Fluorescence light to pass to the sample.

The Digital Camera was turned on, and by using a software program called EOS Utility, the option Remote-Shooting appeared in the computer screen, and it was selected. The Focus Knob reel of microscope has been set to an appropriate and perfect degree, which gives a high-resolution image, including the details of the objects in the monitor screen.

4.12. Biomarker analysis

The preparation of samples for the biomarker analysis method was already done by first grinding the small rock samples into powder, then these powder samples were carefully handled and stored in small bags to prevent contamination, and also the information for each sample was saved as a data.

After that, each of powder sample got the scientific treatment at the (Czech Geological Survey in Brno city, Czech Republic) such as writing the sample name and its properties including the location and other data.

The first remediation of biomarker analytical technique was successfully done by processing each of the samples with 93% of Dichloromethane and with 7% of Methanol, and it was done by using the Dionex ASE100 device, which is a laboratory equipment designed to accelerate and speed up the solvent-extraction process in the laboratory, and this device is also used to extract organic compounds from solid samples, such as sediment rocks, soil, and other various samples.

After the previous solvent-extraction process or method, the fractions of saturated hydrocarbon (SAT) and aromatic hydrocarbon (ARO) were perfectly separated on silica column with using elution by Hexane and Dichloromethane (DCM).

Then, the next step was to analyze both fractions, the saturated hydrocarbon (SAT) and the aromatic hydrocarbon (ARO) by using Agilent A6890N chromatograph equipped with Agilent 5973 NMSD quadrupole mass spectrometer (GC–MS) with using (He) as a carrier gas.

Figure 15: Agilent A6890N chromatograph equipped with Agilent 5973 NMSD quadrupole mass spectrometer (GC–MS)

Additional detail, is the fact that the North Sea oil (NSO) of NIGOGA was used during the laboratory experiment as a reference sample. Finally, for the (m/z 57) Mass-Chromatograms (alkanes and isoprenoids), the (m/z 191) Mass-Chromatograms (terpanes), and the (m/z 217) Mass-Chromatograms (steranes), they were all evaluated and predestined successfully in the laboratory by using the Agilent-MassHunter computer software.

5. Chapter 5: Results

5.1. Gamma-ray spectrometer at the selected outcrop sections.

The data of using gamma-ray spectrometer equipment for each layer at the field was collected and a table was then created by using the MS-Excel software, and its result showes the concentrations of K with unit of (%), U with unit of (ppm), and Th with unit of (ppm), since K, U, and Th can give a good indication of the composition for the formations that were studied, due to the fact that they are naturally radioactive materials which can be recorded commonly inside the earth's layers but with different value based of the formation itself.

For the first section Velka Chuchle, there were 21 recorded layers, starting from the height of 0 m, 0.25 m, 0.5 m, 0.75 m, 1m, until the final layer with height of 5 m, which its own number is layer 21, so recorded log data contains information about (K in%, U in ppm, Th in ppm), so an excel sheet table was created and other calculations were also made such as the computed gamma ray CGR, and SGR, both with unit of (API), including U/Th in unit (ppm) which is used for finding the average concentrations of each layer.

The (Computed Gamma Ray) CGR is a standard method used to estimate the number of various radioisotopes present in a formation. In this project, the isotopes of potassium (K), uranium (U), and thorium (Th) are the most common used examples.

The equation CGR = (Th3.93) + (K16.32), was used to estimate the total gamma ray in the formation, and these units (3.93 for Th and 16.32 for K) are the standard unit of gamma radiation used in the oil and gas industry that miust be measured in the API (American Petroleum Institute) units.

Table 1: Velka Chuchle section Gamma-ray data, from field.

Height (m)	DR (ppm)	K (ppm)	U (ppm)	Th (ppm)	CGR (API)	SGR (API)	U/Th (ppm)
0	30.2	0.5	3.1	2.4	17.59	45.182	1.29167
0.25	25.6	0.4	2.3	2.7	17.14	37.609	0.85185
0.5	29.1	0.4	3.1	2.3	15.57	43.157	1.34783
0.75	24.4	0.3	2.8	1.7	11.58	36.497	1.64706
1	24.3	0.4	2.7	1.9	14	38.025	1.42105
1.25	26.7	0.4	2.8	2.4	15.96	40.88	1.16667
1.5	14.8	0.3	1.3	1.6	11.18	22.754	0.8125
1.75	22.7	0.5	1.9	2.3	17.2	34.109	0.82609
2	23.5	0.5	1.4	3.3	21.13	33.589	0.42424
2.25	26.4	0.7	1.4	3.3	24.39	36.853	0.42424
2.5	21.9	0.8	0.7	2.9	24.45	30.683	0.24138
2.75	19.8	0.6	1	2.6	20.01	28.91	0.38462
3	19.9	0.7	0.6	2.8	22.43	27.768	0.21429
3.25	23.6	0.6	1	3.6	23.94	32.84	0.27778
3.5	30.3	0.7	1.9	4.1	27.54	44.447	0.46341
3.75	24.2	0.5	1.4	3.7	22.7	35.161	0.37838
4	24.5	0.7	1.1	3.6	25.57	35.362	0.30556
4.25	22.3	0.7	1.3	2.5	21.25	32.819	0.52
4.5	26.1	0.8	0.4	5.1	33.1	36.659	0.07843
4.75	24.8	0.7	1.1	3.4	24.79	34.576	0.32353
5	27.6	0.7	1.7	3.7	25.97	41.095	0.45946
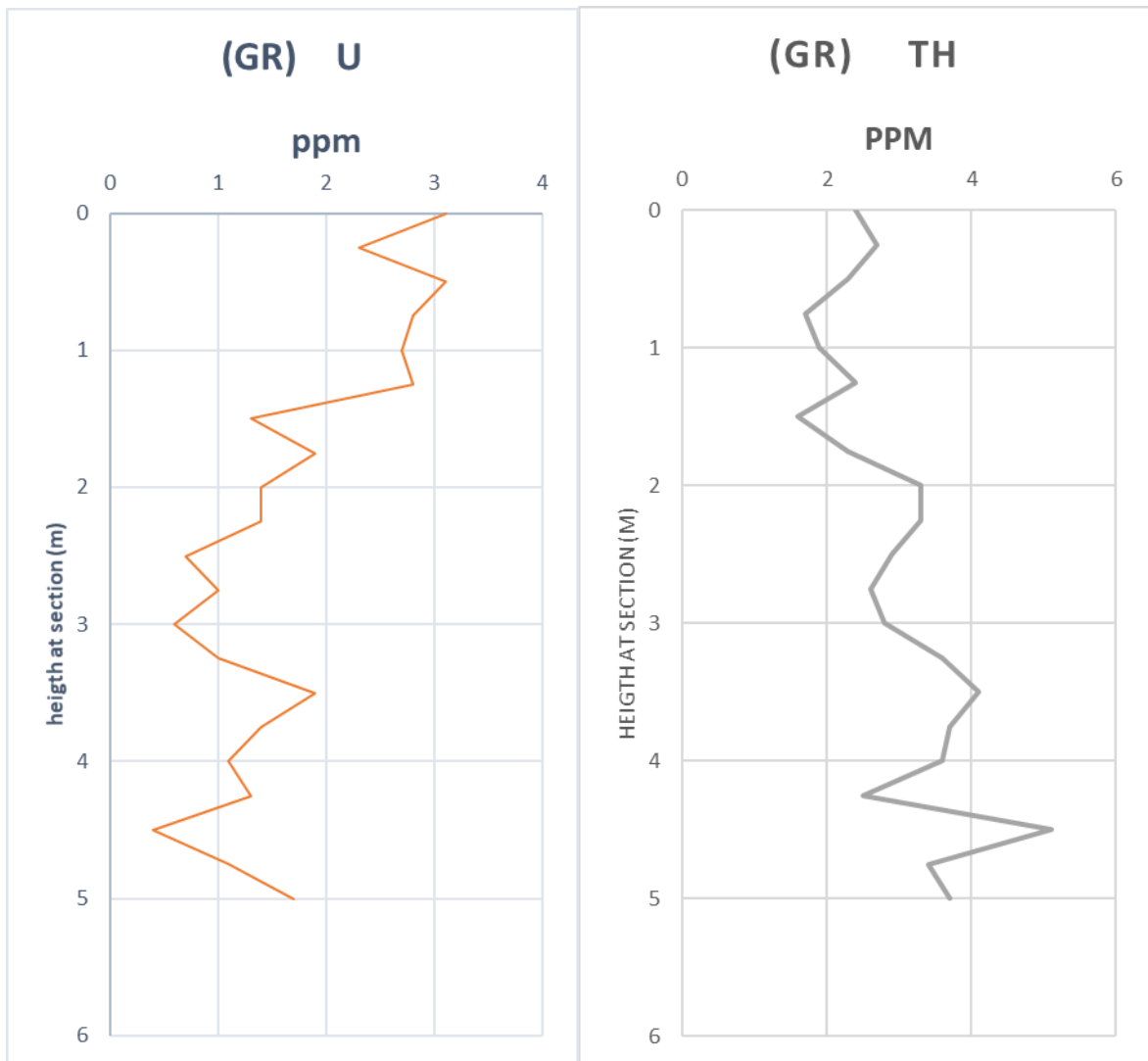
Figure 16: (This is for figger do not forget it A chart that was created using line-chart in Excel, which represents the Gama-Ray logging results, for each layer as it is showing below.

The spectral gamma ray log was displayed in three track records starting with uranium, thorium, and potassium. For the numbers from (0m) to (6m) are representing the height of layers for the location in meter, therefore the number (0m) is the underlying layer, and then increasing each 1 meter.

It can be also noticed that each layer has a different value of radioactivity. For example, the value of (U) Uranium radioactivity decreases as the height of layers increase. On the other hand, the value of (Th) Thorium radioactivity increases as the height of layers increased

30
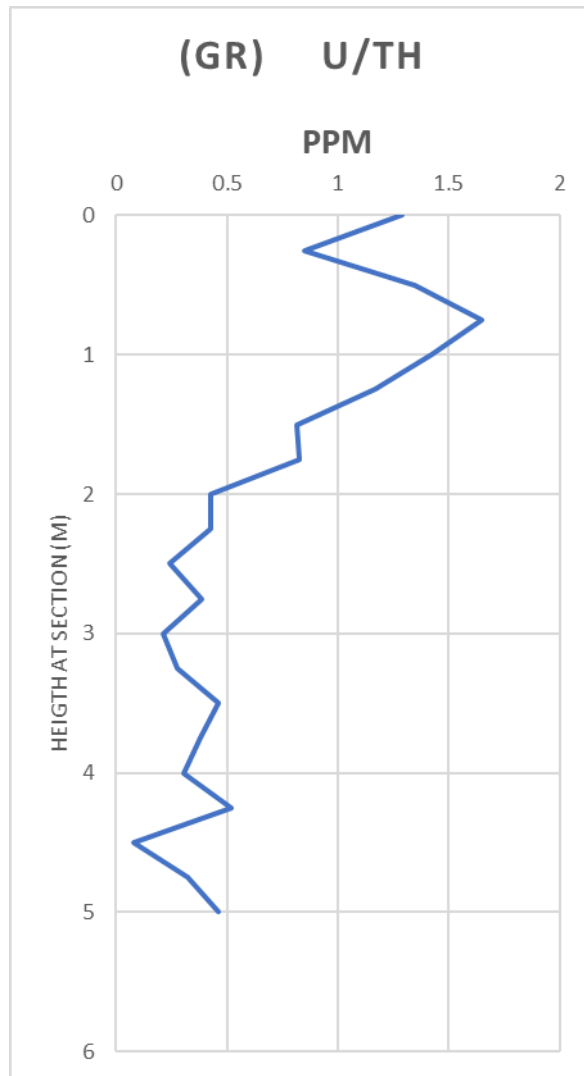
Figure 17: log chart of U/Th

This log-chart of U/Th ratios shows high U/Th ratios in the lower part of the section (0 m to 1.75 m), which is followed by low U/Th ratios in the upper part of the section (2 m to 5 m).
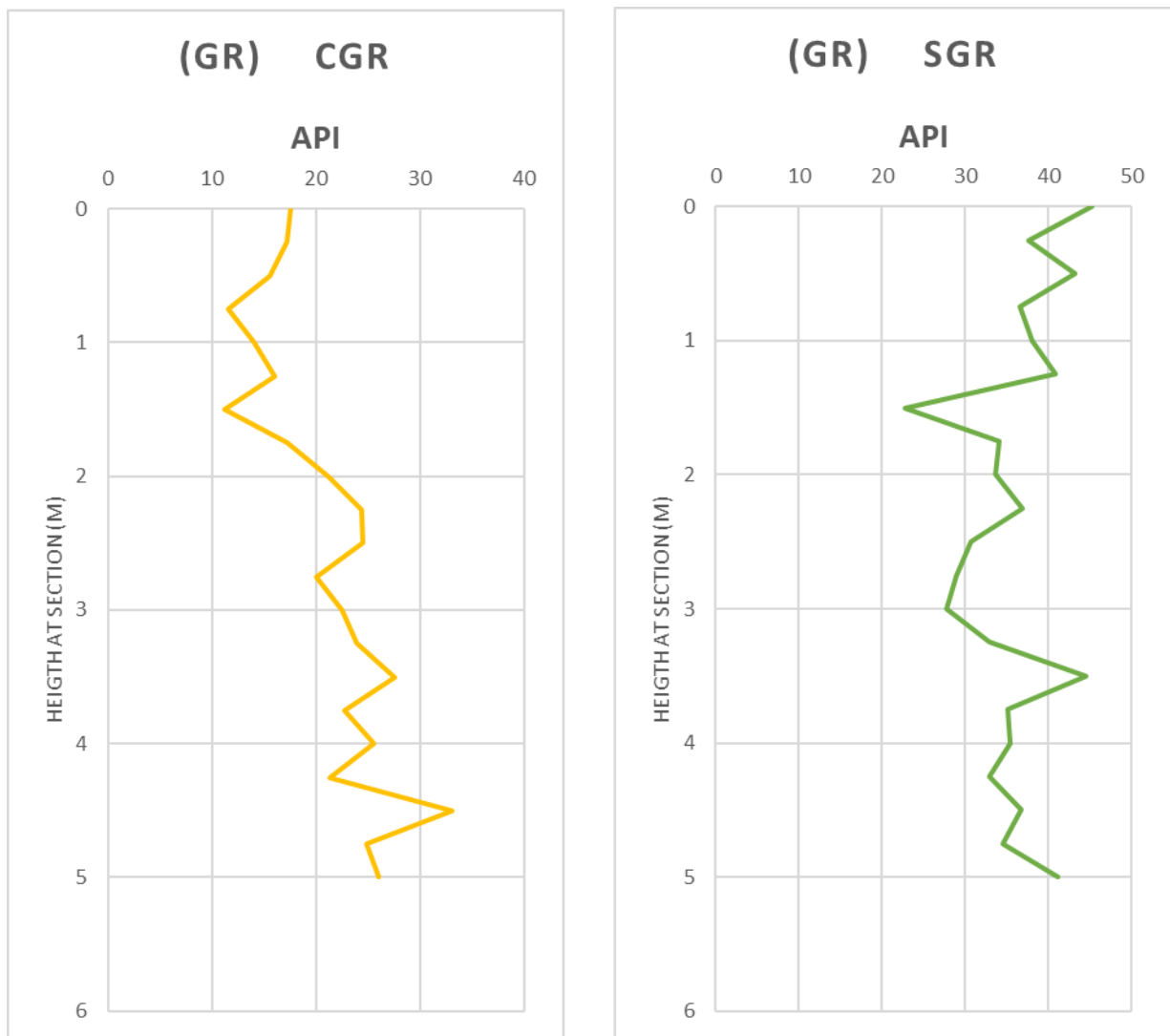
Figure 18: Gamma Log chart, made by Excel and it shows the SGR and CGR

It was used to get the final value for the SGR (API). It shows that the first layer with (0m) meter, has 45 API, which is the highest value, while the layer with (1.5m) has almost the lowest value which is recorded as 22 API.

For the second location (Na Chlumu Quarry), the gamma ray detection device on also was used on the surface of each marked point that and has already prepared from the first step of methodology, and the same process was used for all the layers, so the measurement of the Potassium (K) in % unit, Uranium (U), and Thorium (Th) in PPI unit, were all recorded for each layer.

32

After waiting for 3 minutes, the data as a results of the K/U/Th unstable isotope were recorded and calculated to show the information about the contents for each marked-point in each layer, then another data table was created by using the MS-Excel software

Figure 19: Table of the gamma ray data for Na Chlumu section

height (m)	DR (ppm)	K (ppm)	U (ppm)	Th (ppm)	CGR (API)	SGR (API)	U/Th (ppm)
0	14.9	0.1	2	0.9	5.169	22.969	2.22222
0.5	11.6	0.2	1.3	0.8	6.408	17.978	1.62500
1	7.8	0.1	0.8	0.7	4.383	11.503	1.14286
1.5	14.5	0.2	1.6	1.3	8.373	22.613	1.23077
2	7.8	0.1	0.8	0.7	4.383	11.503	1.14286
2.5	11.7	0.1	1.2	1.3	6.741	17.421	0.92308
3	9.6	0.2	1.1	0.4	4.836	14.626	2.75000
3.5	12.3	0.1	1.5	0.9	5.169	18.519	1.66667
4	6	0.3	0.2	0.6	7.254	9.034	0.33333
4.5	5.5	0.1	0.4	0.7	4.383	7.943	0.57143
5	7.2	0.1	0.5	0.9	5.169	9.619	0.55556
5.5	7.2	0.1	0.5	1.2	6.348	10.798	0.41667
6	7.4	0.1	0.6	1.1	5.955	11.295	0.54545
6.5	6.9	0.1	0.5	0.9	5.169	9.619	0.55556
7	8.6	0.1	0.8	1	5.562	12.682	0.80000
7.5	8.5	0	0.8	1.2	4.716	11.836	0.66667
8	7.1	0.1	0.8	0.8	4.776	11.896	1.00000
8.5	7.7	0.1	0.7	1	5.562	11.792	0.70000
9	6.8	0.1	0.6	0.7	4.383	9.723	0.85714
9.5	16.3	0.2	1.9	1.4	8.766	25.676	1.35714
10	11.6	0.1	1.5	0.6	3.99	17.34	2.50000
10.5	10.8	0.1	1.4	0.8	4.776	17.236	1.75000
11	11.3	0.1	1.4	0.9	5.169	17.629	1.55556
11.5	12.6	0.1	1.6	1.1	5.955	20.195	1.45455
12	10	0.1	1.4	0.5	3.597	16.057	2.80000
12.5	10.5	0.1	1.2	1	5.562	16.242	1.20000
13	15.5	0.1	2	1.3	6.741	24.541	1.53846
13.5	16.5	0.2	1.8	1.8	10.34	26.358	1.00000
14	17.1	0.2	2.1	1.3	8.373	27.063	1.61538
14.5	15.6	0.1	2	1.2	6.348	24.148	1.66667

15	16.5	0.1	2.1	1.4	7.134	25.824	1.50000
15.5	17.8	0.1	2.6	0.7	4.383	27.523	3.71429
16	17.3	0.2	2.2	1.2	7.98	27.56	1.83333
16.5	21.5	0.1	3.3	0.7	4.383	33.753	4.71429
17	24.6	0.2	3.4	1.5	9.159	39.419	2.26667
17.5	27.5	0.2	3.5	2.1	11.52	42.667	1.66667
18	21	0.2	2.7	1.5	9.159	33.189	1.80000
18.5	30.6	0.2	4.4	1.6	9.552	48.712	2.75000
19	27.6	0.2	3.8	1.6	9.552	43.372	2.37500
19.5	22.9	0.3	3.1	1	8.826	36.416	3.10000
20	30.7	0.2	4.3	1.5	9.159	47.429	2.86667
20.5	33.8	0.1	5.1	1.7	8.313	53.703	3.00000
21	27.7	0.2	3.5	2.2	11.91	43.06	1.59091

For this location, Na Chlumu Quarry, a line graph was also created using the Excel chart based on the data from the field, which represents the gamma-ray log, for each layer. The spectral gamma ray log was created in three track records starting with U, Th, and K. The numbers represent the height of the layers (The second location, Na Chlumu Quarry section) from (0m) to (21m).

The number (0m) is the Underlying Layer, and then it is increasing each 1 meter, so based on the chart it can be noticed that each layer has a different value of (U, Th, and K) radioactivity. For example, the radioactivity value of (Uranium in the unit ppm) obviously increases strongly as the height of layers is increased. However, the value of (Thorium in the unit ppm) slowly increases as the height of layers is increased.
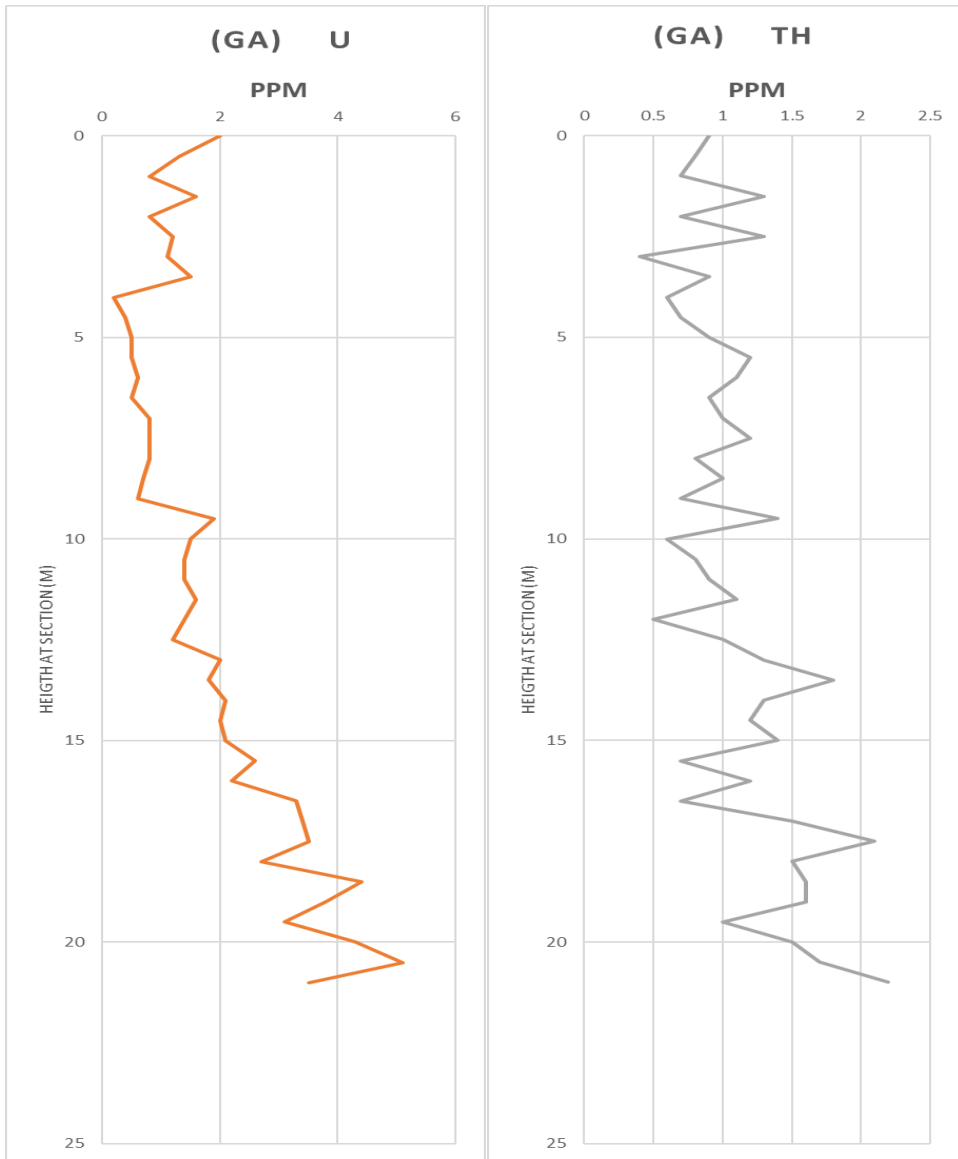
Figure 20: showing the log data graph of U, Th by gamma ray

For this log-chart of U/Th, the line-graph shows the relationship between the data of Uranium radioactive decay divided by Thorium radioactive decay, and it provides the average rang about the radiation of both U & Th in all layers.

It is starting from the first layer (Underlying Layer) with number 0 m, to highest layer with number 25m.

It shows that the layer with almost point 4meter, has a very few radioactivity average range, about (0.33 ppm), while the layer with 16.5m has almost the highest

radioactivity average rang which is recorded as (4.71 ppm). Generally, the radioactivity average range U/Th starts to increases as the height of layers is increased.
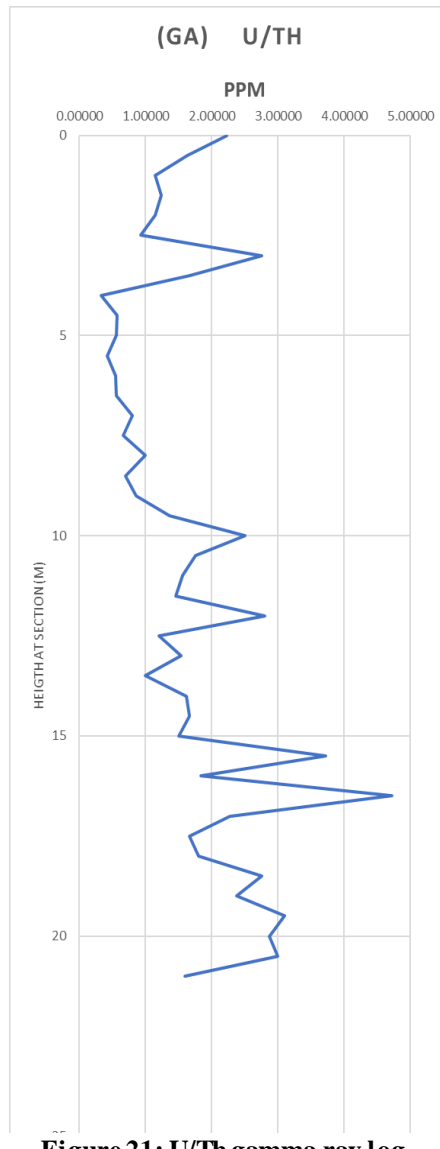
Figure 21: U/Th gamma ray log

This chart shows the gamma log recorded data as a final result of converting field radioactivity data to a log track (graph), for both measurements (Computed Gamma Ray) CGR and the (Standard Gamma Ray) SGR, based of the recoded value of each layer.

The chart of CGR, shows the relationship between (Th ppm) multiplied by (3.93), which then added to the value of (K ppm) that should be multiplied by (16.32), for all of the layers. Therefore, the formula: =(Th*3.93) + (K*16.32) was used for this

calculations, and its numbers or values are standard gamma ray calculations values by the (American Petroleum Institute).
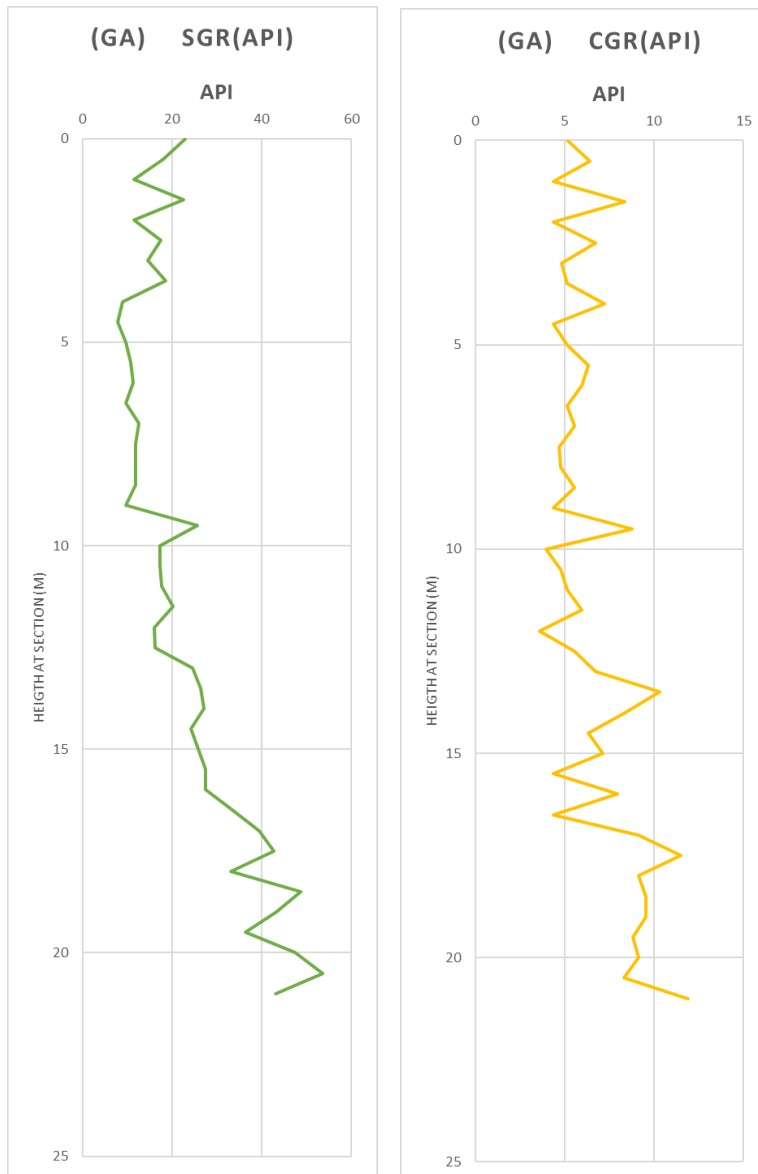
Figure 22: Gamma ray log for SGR and CGR

However, for the (Standard Gamma Ray) SGR, it was calculated by using the total gamma-ray that can be detected from all the radioactive sources in the layers.
The chart below of the SGR, represents the line-graph of the relationship between (Th ppm) Thorium, (U ppm) Uranium, and (K %) Potassium, radioactive values that were

already recorded from the field for all the layers, then another special SGR formula was used for its calculations=(Th*3.93) + (K*16.32) + (U*8.9), which its values are also standard gamma ray values by the (American Petroleum Institute).

5.2. Porosity and permeability measurements

The mesurements of Porosity and Permeablility for each core-plug samples of both locations (Na Chlumu Quarry) section, and (Velka Chuchle) Section, are considered as the most important rock properties that can describes and give information about the ability of the rocks itsealf to hold fluids.

For the porosity (in unit %) measurements and calculations, all of the core-plugs samples were put inside an equipment in the laboratories called a Porosimeter (for measuring Porosity) and it could measure successfully the length, diameter of each core sample including the pore volume and the total porosity itself, and been calculated.

For the permeability (in unit mD) measurements that was done by using gas permeameter device, where core plugs were put inside its chumber and the device startedthe calculations and measurements injecting gas as a fluid.were successfully recorded and it can be noticed that the Prosity precentage of the location (Velka Chuchle) samples are higher than the Prosity precentage of the location (Na Chlumu Quarry) samples.

Table 2: Porosity and Perm(mD) results from lab work

Core ID	Diameter	Length	Porosity %	Perm(mD)
NC 0.5	3.55	5.18	6.360986	2.5
NC 20.5	3.55	5.95	8.345832	2.25
NC 13	3.55	6.7	8.027654	0.8
NC 10	3.55	6.05	7.293865	2.23
NC 3.1	3.55	6.5	6.544377	2.21
NC 15.5	3.55	6.8	6.64963	2.49
NC 19	3.55	5	6.551194	2.51
VCH 3.7	3.55	6.67	8.682386	1.8
VCH 3.1	3.55	5.67	8.329274	0.82
VCH 0.7	3.55	5.98	8.176558	2.15
VCH 2.1	3.55	5.2	9.150057	2.2
VCH 0.5	3.55	4.4	9.26798	2.05
VCH 4.9	3.55	5.1	9.441505	1.9

5.3. Fluorescence microscopy for thin-sections

The fluorescence microscopy gave a signiftienint vew regarding the organic matter inside each sample, for both locations. The first slide with name A, sample NC 0.5 (scale 2.5X, 0.2mm), a veins that cuts the rock and filled with calcite, while slide with number 1, shows the fluorescence view which means organic or any hydrocarbon is not existed in this area, but the silde with name B, sample NC 3.1 (scale 6.3X, 0.2mm), is packstone cut by stylolite, and in the silde with number 2 has a littile brownish color inside the stylolite which means it is filled with hydrocarbon, and the slide with name C, sample NC 10.0 (scale 6.3X, 0.2mm) is packstone with fossils, fragments, but the slide 3 shows no organic matter for this area of the thin-section sampel

Figure 23: 1.1. Fluorescence microscopy for thin-sections for sample NC 0.5

This thin-section sample below is named VCH 4.9, its first slide with name A (with ocular scale 6.3X, 0.2mm), shows wackstone cut by stylolite, and the fluorescence view of silde 1 shows that it has some hydrocarbon by the brownish color inside. The silde B (with ocular scale 6.3X, 0.2mm), is packstone cut by stylolite as well, but in the silde 2, it is not very yellowish or brownish color which means not hydrocarbon.

Finally, slide C (with ocular scale 2.5X, 0.2mm) is contains of wackestone, Echinoderms, ostracod (or mollusc) fragments, with fossils, micrite, and also cut by stylolite with fragments of shells, and also cut by stylolite but has not organic matter as the slide 3 shows no yellowish or brownish color
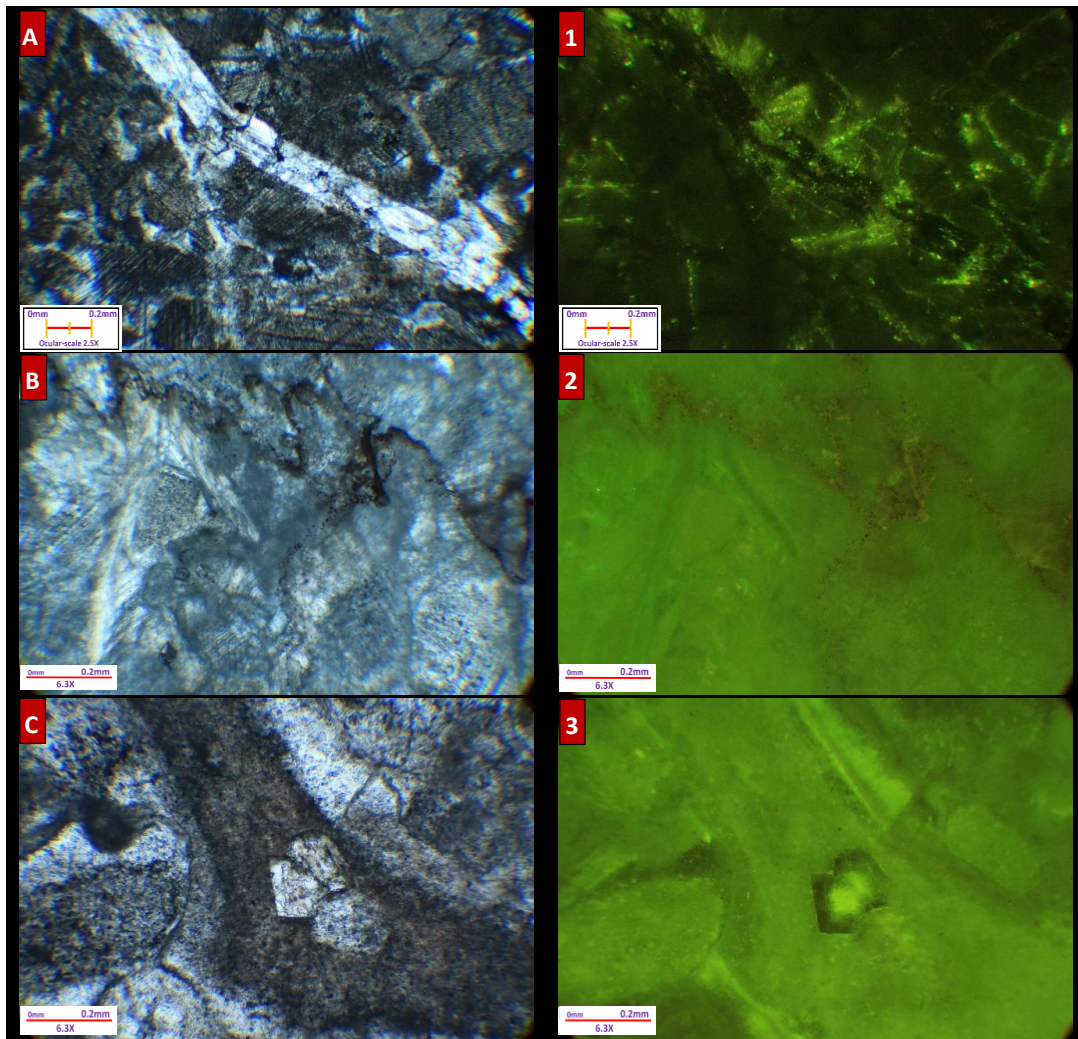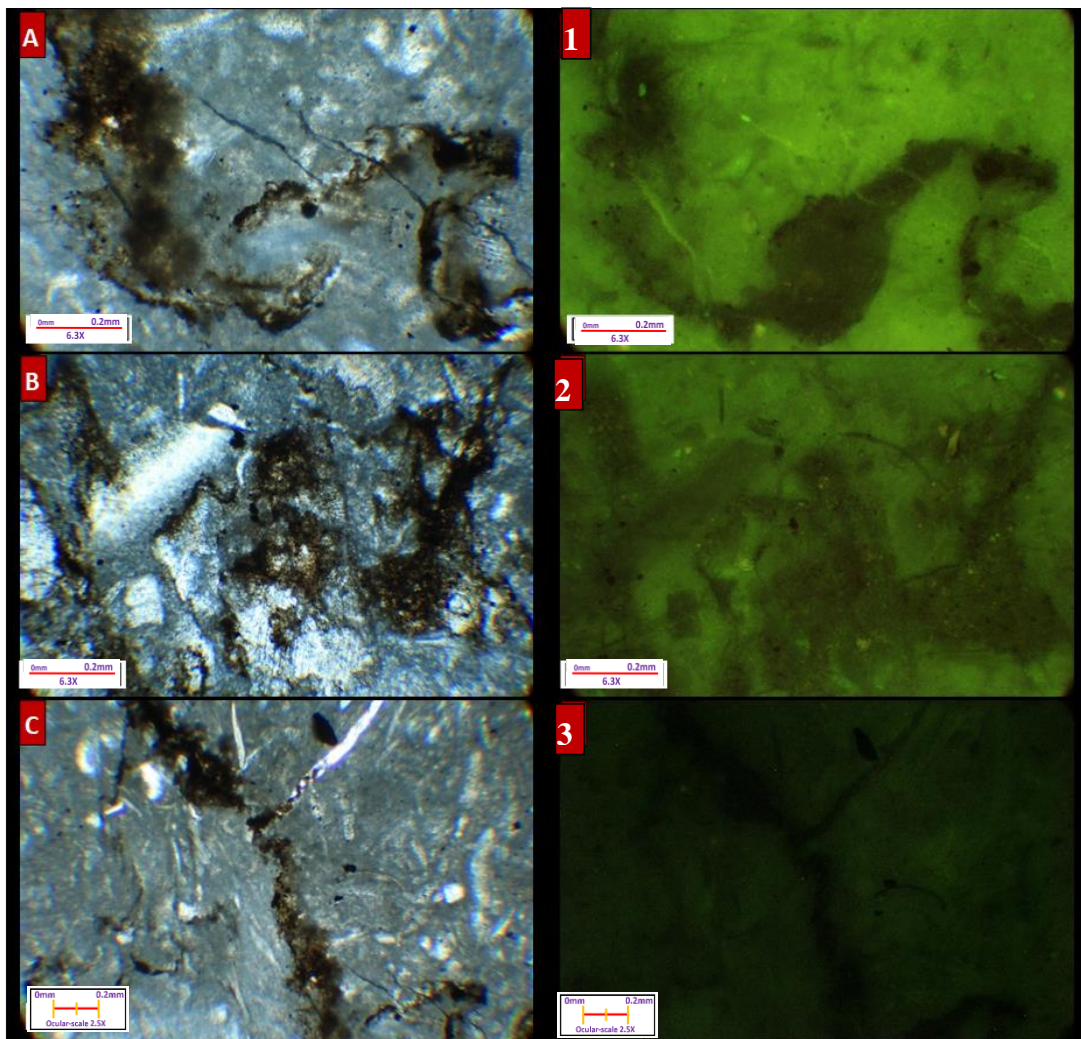

Figure 24: 1.1. Fluorescence microscopy for thin-sections sample VCH 4.9

The thin-section sample below is named VCH 3.1, so the first slide with name A (with scale 6.3X, 0.2mm), shows wackstone cut by stylolite, and the fluorescence view of silde 1 shows that it has a lot of hydrocarbon by the yellowish color inside. The silde B (with ocular scale 6.3X, 0.2mm), is packstone cut by stylolite as well, but in the silde 2, it is small yellowish color which means a very littile hydrocarbon, and the greenish color is from the glue material during the preparing of thin section.

Finally, slide C (with ocular scale 2.5X, 0.2mm) is contains of wackestone, micrite, and the slide 3 shows however no yellowish color or any hydrocarbon.
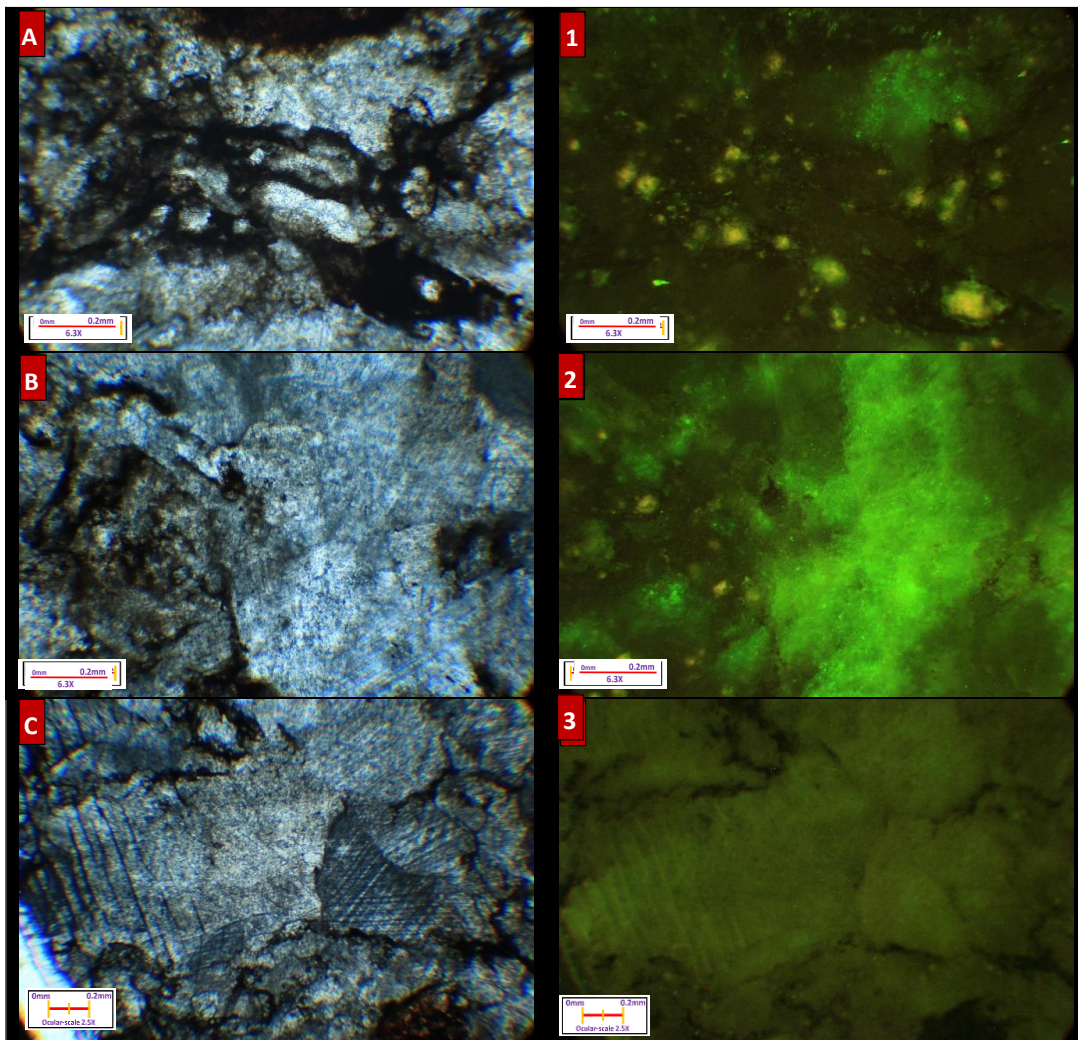
Figure 25: 1.1. Fluorescence microscopy for thin-sections sample VCH 3.1

5.4. Micromorphology analysis results for thin section

The icromorphology analysis is important for the geological thin section analyizing, it tells important information about the formation and the substances it contains, so the results of this type of analysis in this project were important and it was achived very well.

For the section A, sample (NC 3.1), and slide D, (NC 0.5), containing a wackestone cut by calcite vein with fibrous cement. Slide B, sample (NC 10.0), and slide F, (NC10.0) containing a wackestone, micrite cut by a stylolite and filled with organic matter (migrated hydrocarbons). Slide C, (NC 0.5), could be a brachiopod / bivalve shell in the centre. Slide E, (NC10.0), is packstone filled with microorganisms.

Figure 26: 5.4. Micromorphology analysis for NC 0.5
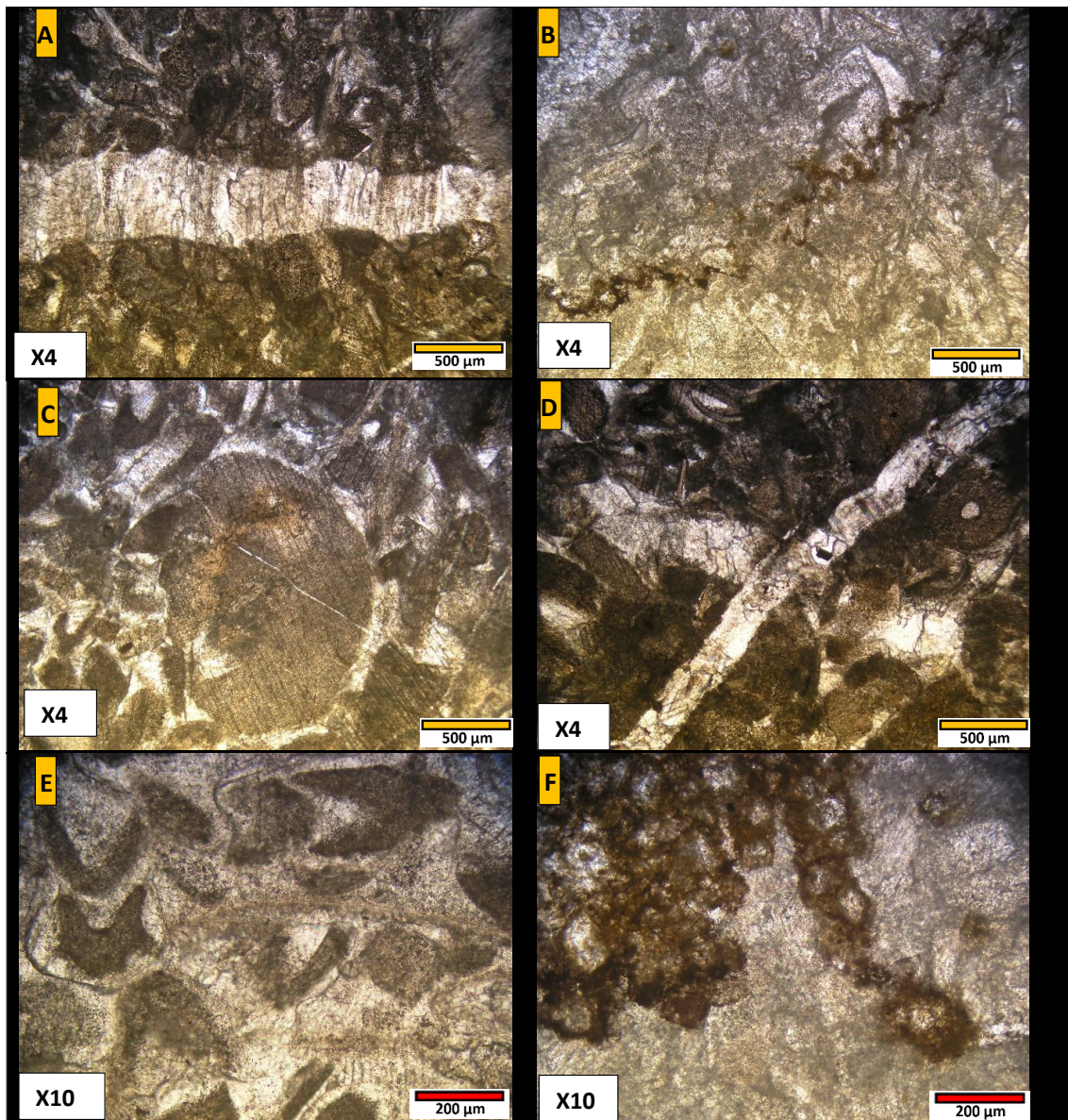
For slide A, slide B, and slide C, (sample name VCH 3.1) they are all containing micrite cut by a veins, and filled with calcite, but for A&C they are also cut by stylolite that is filled with some organic matter (migrated hydrocarbons). For D slide is wackestone cut by calcite vein with fibrous cement and surrounding by thick stylolite filled with hydrocarbon. For E&F slides are packstone cut by calcite large fibrous cement, then cut by stylolite with hydrocarbon.
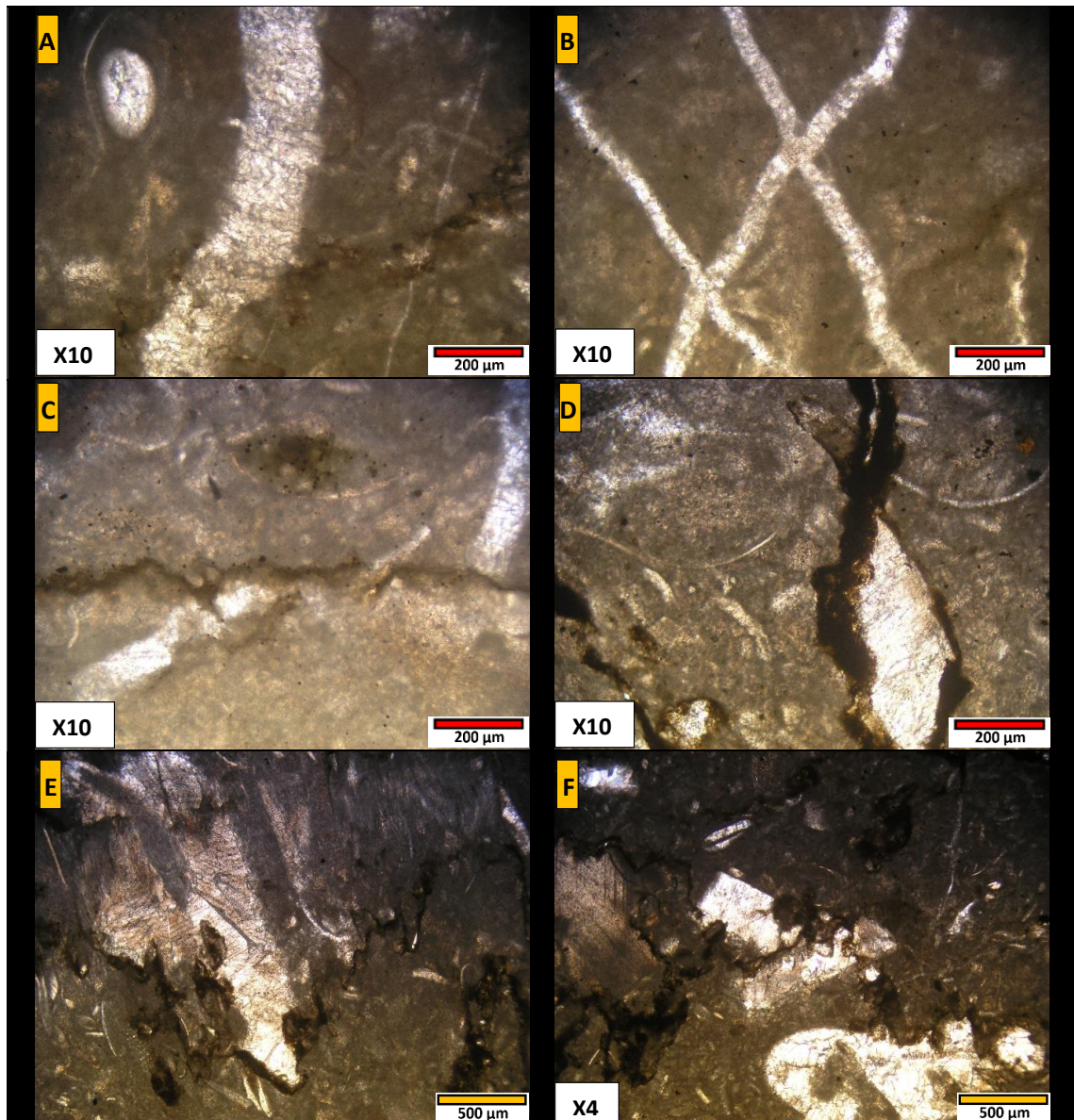
Figure 27: 5.4.   Micromorphology analysis for many samples written in the text

The photomicrographs of the thin section (VCH 0.5) (with both objective lenses X10 & X4), and for slides A, B, they are wackestone containing micrite, in middle of slide B it is cut by calcite vein with fibrous cement, and for C,E and D slide is micrite, with small stylolite, while for F slide, it is packstone with few fossils, fragments of shells.
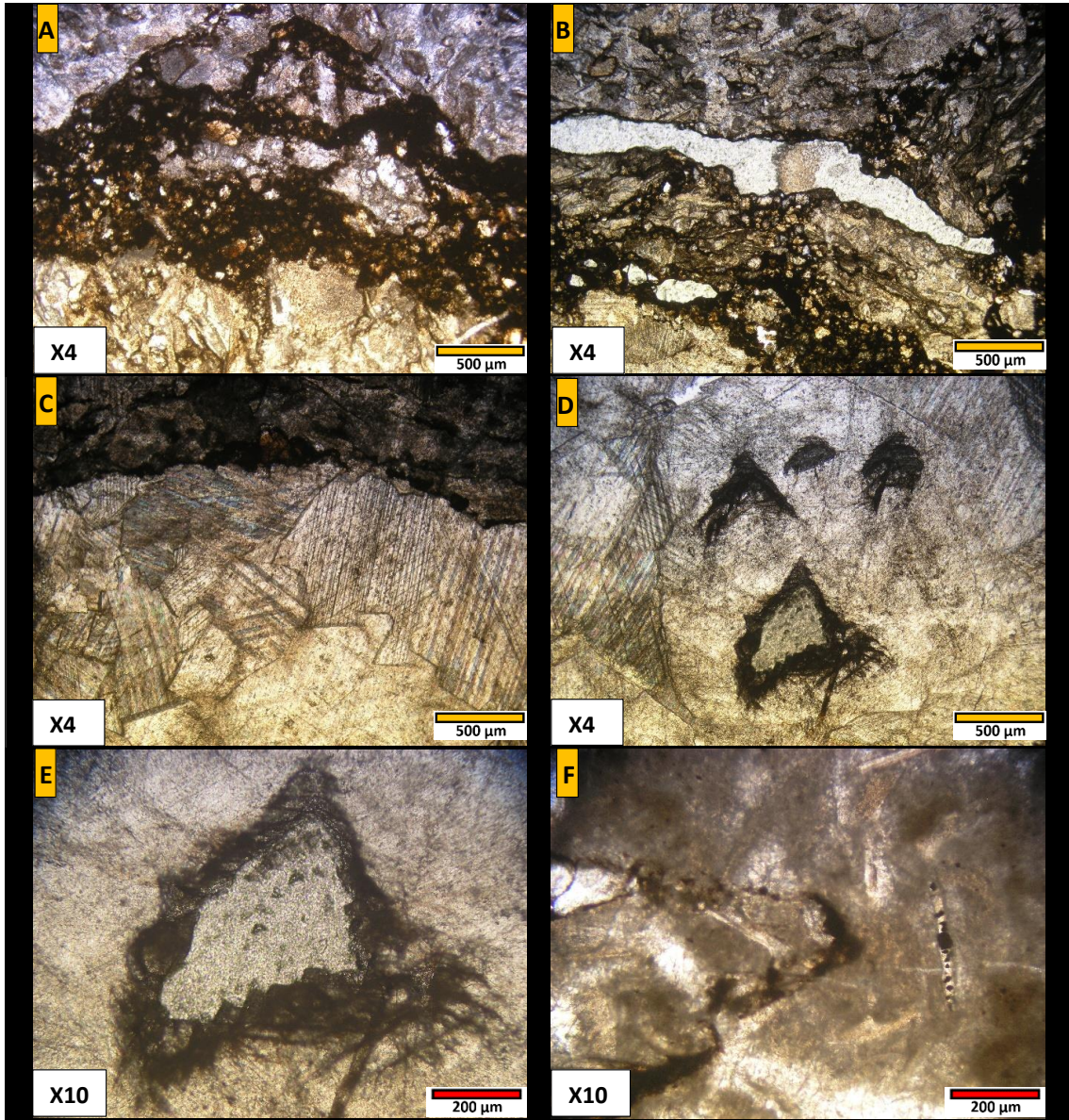
Figure 28: 5.4.   Micromorphology analysis for VCH 0.5 sample

5.5. TIC, TOC and TS analysis

N	Evidence CL-number	Samples-code	TIC % (m/m)	TOC % (m/m)	TS % (m/m)
1	2310176	NC 0,5	11.72	<0,05	<0,05
2	2310177	NC 3,1	11.59	0.17	<0,05
3	2310178	NC 10	11.09	0.64	<0,05
4	2310179	NC 13	11.65	<0,05	<0,05
5	2310180	NC 15,5	11.78	<0,05	<0,05
6	2310181	NC 19	11.40	0.25	<0,05
7	2310182	NC 20,5	11.06	0.32	<0,05
8	2310183	VCH 0,5	11.39	<0,05	<0,05
9	2310184	VCH 0,7	11.59	0.07	<0,05
10	2310185	VCH 2,1	11.10	0.24	<0,05
11	2310186	VCH 3,1	11.48	<0,05	<0,05
12	2310187	VCH 3,7	11.33	<0,05	<0,05
13	2310188	VCH 4,9	11.14	<0,05	0.24

Table 3: TIC, TOC TS, mesurments for carbon

Based on the results, the values of (TIC) for each layer and each sample ranged from about 11.06% (m/m) to 11.78% (m/m). This means that every sample gathered has a large amount of artificial carbon.

On the other hand, the (TOC) readings were very low. For example, in a few samples (NC 0.5, NC 13, NC 15.5, VCH 0.5, VCH 3.1, and VCH 3.7), less than (0.05% m/m) of the Total Organic Carbon (TOC) was already found.

Total organic carbon (TOC) amounts in samples that were tested ranged from 0.07% to 0.64%. This means that there was organic carbon in the samples, which could have come from plants or animals.

5.6. Biomarker

6. Table 4: Results of Biomarker analysis

| N	CGS No.	Kód vz.	Depth (m)	Pr/ Phy	Pr/n-C17	Phy/n-C18	(Pr/n-C17)/ (Ph/n-C18)	n-C17/(n-C17 + n-C27)	% Norpr	% Pr	% Ph
1	2310177	NC 3,1	Na Chlumu lom 3,1 m	0.908	0.938	0.504	1.861	0.222	16.503	39.740	43.757
2	2310178	NC 10	Na Chlumu lom 10 m	1.204	0.988	0.496	1.992	0.499	23.129	41.994	34.876
3	2310181	NC 19	Na Chlumu lom 19 m	1.573	0.605	0.313	1.934	0.669	30.983	42.195	26.822
4	2310182	NC 20,5	Na Chlumu lom 20,5 m	2.503	0.499	0.236	2.117	0.847	39.052	43.548	17.401
5	2310184	VCH 0,7	Velká Chuchle 0,7 m	1.429	0.579	0.273	2.120	0.295	22.249	45.740	32.011
6	2310185	VCH 2,1	Velká Chuchle 2,1 m	2.451	0.401	0.166	2.412	0.800	36.192	45.319	18.489

CPI-1(n-C25..33)	CPI-2	CPI-3 (2*C29/ (C28+C30))	CPI (C26+C27)/ (C25+C28)	n-C15 /n-C20	n-C30 /n-C20	n-C15 /n-C17	n-C12 /n-C15	n-C31 /n-C19	mid chain OEP
1.160	1.142	1.251	1.063	0.064	0.567	0.206	0.592	0.925	0.986
1.472	1.452	1.683	1.155	0.225	0.379	0.247	0.745	1.022	1.006
1.374	1.321	1.446	1.167	0.720	0.353	0.413	0.140	0.679	1.001
1.340	1.280	1.386	1.144	2.233	0.229	0.666	0.027	0.281	0.970
1.065	1.035	1.032	1.049	0.132	0.514	0.299	0.065	0.572	0.978
1.073	1.062	1.027	1.000	1.412	0.211	0.981	0.062	0.192	0.991

After the previous solvent-extraction process or method, the fractions of saturated hydrocarbon (SAT) and aromatic hydrocarbon (ARO) were perfectly separated on silica column with using elution by Hexane and Dichloromethane (DCM). Next step, was to analyze both fractions, the saturated hydrocarbon (SAT) and the aromatic hydrocarbon (ARO) by using Agilent A6890N chromatograph equipped with Agilent 5973 NMSD quadrupole mass spectrometer (GC–MS) with using He carrier
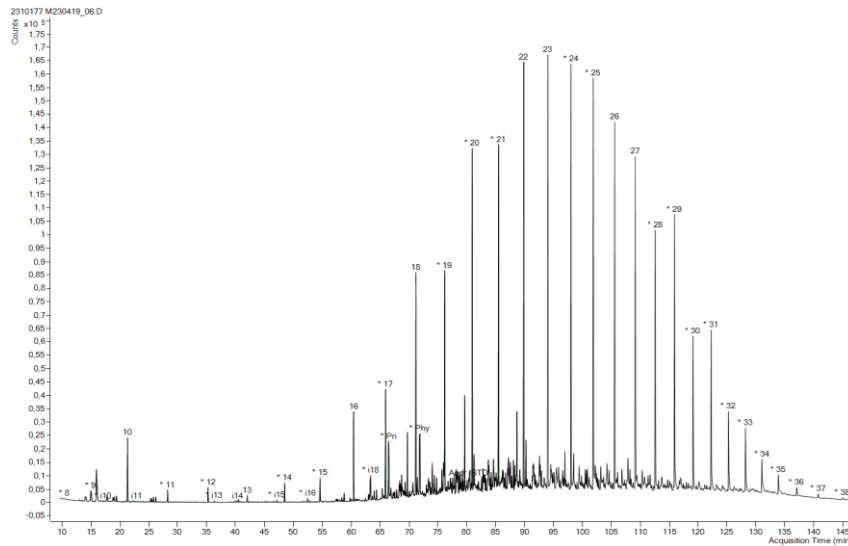
Figure 29: Mass chromatogram m/z 57.sample.2310177/Na Chlumu lom/3,1 m

primitive macrophyta - transition of aquatic to subaeral plants (C23-25).
probably also blue algae (C18-20)   and some contribution by subaeral plants (C29-33)
Pri<Phy. pristane is smaller than phytane, dysoxic to partly anoxic depositional
environment. High odd/even predominance (C28-31 range) means lower maturity
odd/even n-alkanes = close to 1 (C18=19 and C20=21). means lower maturity
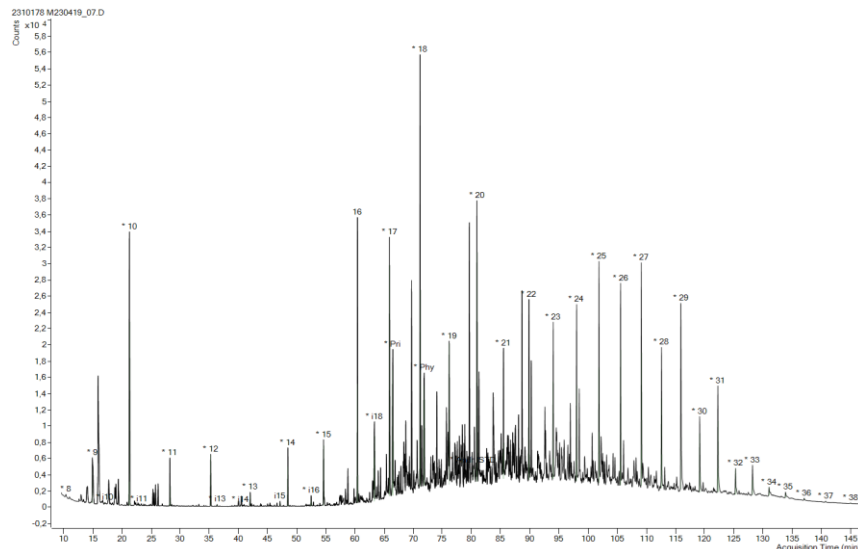
Figure 30: Mass chromatogram m/z 57 sample/2310178/ Na Chlumu lom/10 m

Aquatic similarly abundant to subaeral (terrestrial) plant material   Pri>Phy.
Pristane similar to phytane oxic or less oxic depositional environment

47

5.7. X-ray fluorescence) analysis

X-ray Fluorescence (XRF) analysis is a powerful process for identifying the non-organic materials inside powder samples of each layer from both locations and to identify the compositions of the rock, analyzing minerals in all positions in the laboratory, and the results below provided a comprehensive view of the elemental composition of every powder samples.

Table 5: XRay analysis data

Sample	Al (ppm)	Si (ppm)	P (ppm)	S (ppm)	K (ppm)	Ca (ppm)	Ti (ppm)	V (ppm)	Mn (ppm)
NC 0.5	0	8508.68	12529.31	45.95	0	436281.69	216.6	83.19	84.17
NC 3.1	0	8438.8	12615.02	39.88	0	433146.2	171.03	85.02	35.08
NC 10.0	0	8470.56	12249.2	44.76	0	431450.46	177.75	72.94	91.73
NC 13.0	0	8922.93	12787.8	21.74	0	433652.09	283.29	70.84	126.68
NC 15.5	0	9219.42	12610.26	50.29	0	430909.8	270.82	69.65	287.41
NC 19.0	0	9565.01	12882.61	83.98	0	429497.11	328.73	72.23	157.5
NC 20.5	1283.45	10749.03	13409.03	63.67	210.55	428601.78	503.62	131.56	141.45
VCH 0.5	2106	15202.02	12881.38	131.2	791.72	414212.75	450.39	61.72	99.54
VCH 0.7	0	8848.64	12508.27	50.76	0	443664.09	293.11	110.89	94.52
VCH 2.1	2620.7	14745.27	12109.61	143.14	1110.82	405523.53	563.49	90.66	273.28
VCH 3.1	3133.05	17977.31	11904.41	283.25	1466.28	398828.57	593.54	113	268.41
VCH 3.7	2685.82	16662.56	11956.02	150.92	931.08	404806.92	460.3	91.84	438.66
VCH 4.9	3214.98	17224.83	11893.2	512.5	1297.37	394529.35	500.57	105.45	248.89

Sample	Fe (ppm)	Ni (ppm)	Cu (ppm)	Zn (ppm)	As (ppm)	Rb (ppm)	Sr (ppm)	Zr (ppm)	Mo (ppm)	Pb (ppm)	Th (ppm)	LE (ppm)
NC 0.5	0	16.19	0	9.47	0	0	164.14	6.24	4.49	4.39	20.45	529980.11
NC 3.1	0	0	8.28	7.31	0	1.49	190.53	5.9	5.51	5.08	22.31	532391.67
NC 10.0	0	0	8.79	8.81	0	0	173.39	5	4.4	5.01	24.96	540421.69
NC 13.0	92.46	0	0	10.37	0	1.9	185.88	8.39	6.51	5.55	26.54	529633.96
NC 15.5	663.6	19.08	9.89	7.35	2.15	2.15	164.3	6.51	3.55	3.31	20.25	539616.27
NC 19.0	116.8	0	8.44	12.66	0	2.98	170.2	7.24	3.81	6.89	19.05	540070.03
NC 20.5	2385.18	28.74	13.38	21.2	7.54	5.3	193.09	9.24	4.01	7.81	23.1	534402.51
VCH 0.5	1422.59	13.13	18.95	22.84	2.95	6.88	532.82	11.89	5.08	3.66	27.85	542122.9
VCH 0.7	290.08	14.87	12.36	9.04	1.95	1.79	209.01	6.01	3.46	6.3	28.54	526044.59
VCH 2.1	2380.68	0	24.68	19.7	0	9.19	471.98	12.84	3.53	6.6	26.35	553778.64
VCH 3.1	3447.58	0	18.22	15.57	2.22	12.3	411.07	16.04	6.34	9.84	34.12	543807.99
VCH 3.7	2753.04	0	14.97	19.81	0	8.93	444.65	15.14	3.81	7.5	18.14	546730.35
VCH 4.9	5468.52	0	20.98	16.84	0	10.93	385.41	15.69	4.9	10.76	24.04	556917.72

"The below table belongs to the upper table showing more elements"

It can be noticed that there are some elements in the table with very low existence or even do not exist in some of the powder samples, which meants the layers of the field location they were collected from. For, example, both elements (AI) & (K), in unit ppm, share zero (ppm) in formations of layers (NC 0.5, NC 3.1, NC 10.0, NC 13.0, NC 15.5, NC 19.0). The Ni, and Cu are also not exist in the formations of layer (NC 13.0).

The samples NC 0.5, NC 3.1, NC 10.0, also contain very few and limited Iron (Fe) in unite ppm in their formation based on the resulted datat. Hoever, there are elemnts appears very highly in some formations, such as the Calcium (Ca), Phosphorus (P), Silicon (Si), in the layers NC 20.5, NC 0.5, NC 13.0, including most of VCH samples
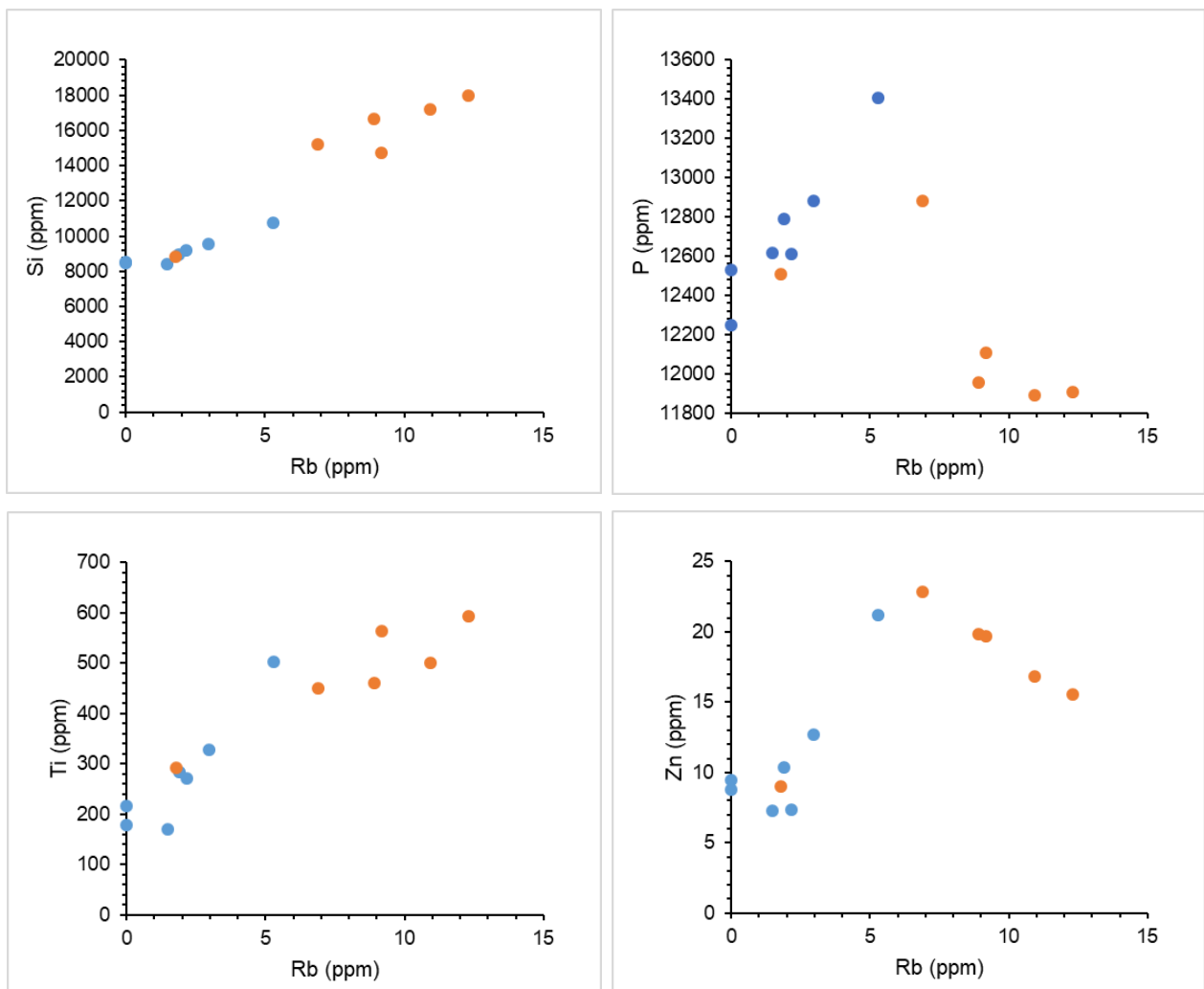
Figure 31: Charts for data of x ray

Chapter 6 Conclusions and Recommendations

6.1. Conclusions

This study's goal is to set the presence, and the existence of bitumen and then correlated and linked it with the stratigraphy and petrology of Lochkov Formation's host carbonates in order to compare it to the overlying of Praha Formation.

Therfore, a lot of scientific procedures and investigations were done for the purpose of any possibility for hydrocarbon existence in the Lower Devonian carbonates of the Prague Basin, in the Czech Republic.

During the experimental works at the laboratory, such as the Micromorphology analysis, as well as the fluorescence microscopy for thin-sections, stylolites where found as conduits for hydrocarbons in abundance, therefor it may play a significant role in migration of hydrocarbon. It is possible to make a comparison with previous research that was carried out in a variety of geological settings where the stylolites were suspected of playing a role in hydrocarbon migration.

However, this study is focusing on comparing between both sections NC and VCH by using total organic carbon (TOC) analysis technique in order to determine the stratigraphic zones that enriched in hydrocarbons in Lower Devonian rocks of the Prague Basin (Lochkov Formation).

Generally, the comparison between Lochkov (lower part of the Prague Basin) and Praha Formation (upper part of the Prague Basin), and so for the Lochkov Formation it corresponds to the Lochkovian stage of the Lower Devonian, also contains Silurian volcanic rocks that erupted in a continental rift setting, contains dark, hemipelagic carbonates and clays that accumulated under dysaerobic bottom-water conditions between turbidite events.

On the other hand, for the Praha Formation, which is pper and lower part of the Prague Basin, it corresponds to the Pragian stage of the Lower Devonian as well as its lithology contains limestones, dolomites, and shales, and contains abundant fossils, including brachiopods, trilobites, and graptolites.

In addition, at the VCH section, the boundary between the Lochkov and Praha Formations is approximately 2.1 meters above the base, whereas, at the NC section, the precise boundary is undetermined.

The Total Inorganic Carbon (TIC), Total Organic Carbon (TOC), are known by showing advantageous details on the composition and quality of different samples.

Therefore, The results of total inorganic carbon (TIC), and total organic carbon (TOC), for the layers samples were successfully measured.

Based on the results, the values of (TIC) for each layer and every sample were vary from approximately 11.06% (m/m) to 11.78% (m/m), so this has indicated that each and every collected sample contains a significant quantity of inorganic carbon.

On the other hand, there were found very low values in the (TOC) readings, such as less than (0.05% m/m) of the Total Organic Carbon (TOC) was already found in a few samples, like NC 0.5, NC 13, NC 15.5, VCH 0.5, VCH 3.1, and VCH 3.7.
It is commomly known that when the values of total organic carbon (TOC) levels in the measured samples varied from 0.07% to 0.64%, this means the existence of organic carbon, which could be generated from plants or animal materials.

In summary, the distribution of organic carbon seems to be unequal among all of the collected samples

In addition, the TS values for the majority of samples were consistently below 0.05% m/m, except for sample (VCH 4.9), which has a TS value of 0.24%, therfore this suggests that the samples contain a low concentration of both organic and inorganic solids. In summary, The samples that were studied had high levels of inorganic carbon and low amounts of organic carbon

Looking forward to future research, perhaps an expanded study area within the Prague Basin can provide a larger picture of the dynamics of the petroleum system. Experimental studies investigating the relationship between cellulite formation and hydrocarbon migration can provide direct evidence

.

References

Bábek, O., Faměra, M., Hladil, J., Kapusta, J., Weinerová, H., Šimíček, D., Slavík, L., & Ďurišová, J. (2018). Origin of red pelagic carbonates as an interplay of global climate and local basin factors: Insight from the Lower Devonian of the Prague Basin, Czech Republic. *Sedimentary Geology*, *364*, 71–88. https://doi.org/10.1016/j.sedgeo.2017.12.007

Kraft, P., Pšenička, J., Sakala, J., & Frýda, J. (2019). Initial plant diversification and dispersal event in upper Silurian of the Prague Basin. *Palaeogeography, Palaeoclimatology, Palaeoecology*, *514*(April 2018), 144–155. https://doi.org/10.1016/j.palaeo.2018.09.034

Mergl, M. (2011). *Earliest occurrence of the Hirnantia Fauna in the Prague Basin (Czech Republic)*. Štěpánek 1984, 63–70. https://doi.org/10.3140/bull.geosci.1245

Šimíček, D., Bábek, O., Faměra, M., & Kalvoda, J. (2020). Million-year secular variations in the elemental geochemistry of Devonian marine records and a link to global climate and bioevents: Prague Basin, Czechia. *Sedimentary Geology*, *402*. https://doi.org/10.1016/j.sedgeo.2020.105651

Vodrážková, S., Kumpan, T., Vodrážka, R., Frýda, J., Čopjaková, R., Koubová, M., Munnecke, A., Kalvoda, J., & Holá, M. (2022). Ferruginous coated grains of microbial origin from the Lower Devonian (Pragian) of the Prague Basin (Czech Republic) – Petrological and geochemical perspective. *Sedimentary Geology*, *438*. https://doi.org/10.1016/j.sedgeo.2022.106194

Volk, H. (2000). Source rock, bitumens and petroleum inclusions from the Prague Basin (Barrandian, Czech Republic) � constraints for petroleum generation and migration from petrology, organic chemistry and basin modelling. *Thesis of the Rheinisch-Westf�lisch-Technische Hochschule Aachen, Faculty for Bergbau, H�ttenwesen Und Geowissenschaften, 338 p.*, 338 pp.

Patočka, F. and Štorch, P. (2004) 'Evolution of geochemistry and depositional settings of early Palaeozoic siliciclastics of the Barrandian (Teplá-Barrandian Unit, Bohemian Massif, czech republic)', *International Journal of Earth Sciences*, 93(5), pp. 728–741. doi:10.1007/s00531-004-0415-6.

Kříž, J., 1991. The Silurian of the Prague Basin (Bohemia)–tectonic, eustatic and volcanic controls on facies and faunal development. Special Papers in Palaeontology, 44, pp.179-203.

Jahn, J.H. (1883) Einige Bemerkungen über das böhmische Silur und über die Bildung des Erdöls. Verhandlungen der k.k. geologischen Reichsanstalt, 16, 372-379.

Chlupáč, I. and Štorch, P., 1992. Regionálně geologické dělení Českého masívu na území České republiky. *Časopis pro mineralogii a geologii*, *37*(4), pp.25-275.

HAVLÍČEK, V. 1981. Developent of a linear sedimentary depression exemplified by thePrague Basin (Ordovician–Middle Devonian; Barrandian area – central Bohemia).Sborník geologických věd, Geologie 35, 7–43.

CHLUPÁČ, I. & KUKAL, Z. 1988. Possible global events and the stratigraphy of the Palaeozoic of the Barrandian (Cambrian – Middle Devonian, Czechoslovakia). Sborník geologických věd, Geologie 43, 83–146.

ŽÁK, J., KRAFT, P., HAJNÁ, J. 2013. Timing, styles, and kinematics of Cambro–Ordovician extension in the Teplá–Barrandian Unit, Bohemian Massif, and its bearing on the opening of the Rheic Ocean. International Journal of Earth Sciences (Geologische Rundschau) 102, 415–433. DOI: 10.1007/s00531-012-0811-2

KUKAL, Z. 1957. Petrografický výzkum letenských vrstev barrandienského ordoviku. Sborník Ústředního ústavu geologického 24(1), 7–112.

Koehn, D., Rood, M.P., Beaudoin, N., Chung, P., Bons, P.D., and Gomez-Rivas, E. (2016) A new stylolite classification scheme to estimate compaction and local permeability variations. Sedimentary Geology, 346, pp. 60-71.

Cháb, J., 2010. *Outline of the geology of the Bohemian Massif: the basement rocks and their Carboniferous and Permian cover*. Czech Geological Survey Publishing House.

VACEK, F. and ŽÁK, J. (2017) 'A lifetime of the Variscan orogenic plateau from uplift to collapse as recorded by the Prague Basin, Bohemian Massif', *Geological Magazine*, 156(3), pp. 485–509. doi:10.1017/s0016756817000875.

Bábek, O., Kalvoda, J., Cossey, P., Šimíček, D., Devuyst, F.X. and Hargreaves, S., 2013. Facies and petrophysical signature of the Tournaisian/Viséan (Lower Carboniferous) sea-level cycle in carbonate ramp to basinal settings of the Wales-Brabant massif, British Isles. Sedimentary Geology, 284, pp.197-213.

Aubrechtova, Martina. (2015). A revision of the Ordovician cephalopod Bactrites sandbergeri Barrande: Systematic position and palaeobiogeography of Bactroceras. Geobios. 10.1016/j.geobios.2015.03.002.

Tissot, B. P., & Welte, D. H. (1984). "Petroleum formation and occurrence". Springer-Verlag. ISBN 978-3-642-87813-87

Horsfield, B. (1989). Practical criteria for classifying kerogens: Some observations from pyrolysis-gas chromatography. 53(4), pp.891–901. doi:https://doi.org/10.1016/0016-7037(89)90033-1.

Hunt, J. M. (1996). "Petroleum Geochemistry and Geology". W. H. Freeman and Compan